

## ARTICLES

## Direct determination of the quantum-mechanical density matrix: Parquet theory

Koji Yasuda

*Graduate School of Human Informatics, Nagoya University, Chikusa-ku, Nagoya 464-8601, Japan*

(Received 1 October 1998)

The methods used to determine the reduced density matrix (RDM) of the ground and excited states, the finite-temperature systems, and the large systems without using the wave function by solving the density equation were discussed. We examined the foundations to reconstruct the higher-order RDMs of the ground and excited states and the finite-temperature systems in terms of the lower-order RDMs. We presented the equation to determine the RDMs of the finite-temperature systems directly and showed that only the exact RDMs satisfy the equation. Our previous approximation for third- and fourth-order RDMs of the ground state [H. Nakatsuji and K. Yasuda, *Phys. Rev. Lett.* **76**, 1039 (1996)] was reformulated, and the accuracy of this approximation for the excited states was examined. The structure of the  $n$ th order energy density matrix ( $n$ -EDM) was analyzed, and the calculation method which sums up the Parquet diagram of the 2-EDM without explicitly constructing the third- and fourth-order RDMs was reported. This approximation is more accurate than the previous second-order approximation and also includes the infinite series of bubble and ladder Green's function diagrams. Such a method is necessary to apply the density-equation method to large systems, such as polymers, metals, and semiconductors. The new approximation together with the density equation was applied to the ground states of some molecules including CO, C<sub>2</sub>H<sub>2</sub>, C<sub>3</sub>H<sub>8</sub>, and C<sub>4</sub>H<sub>10</sub>, and the excited states of the Be atom and Li<sub>2</sub> molecule. The calculated energies were as accurate as the exact or coupled-cluster single and double excitations with triples included noniteratively, and the energy errors of the second-order approximation were significantly reduced. The calculated 2-RDMs almost satisfied important representability conditions while the 1-RDMs were exactly ensemble representable. These results demonstrate that the density equation offers a new quantitative method for treating electron correlations. The relationship between the iterative procedure and the finite-temperature density-equation method was discussed. [S1050-2947(99)07806-3]

PACS number(s): 31.15.Ew, 31.25.-v, 03.65.Ge

## I. INTRODUCTION

Although the wave function has all the accessible information in quantum mechanics, it often tells us more than we need to know. Since all the operators we shall concern ourselves with in quantum mechanics are one- and two-body ones, essential physical quantities can be calculated from the second-order reduced density matrix (2-RDM). If we can determine it without using the wave function, the wave function can be eliminated from the quantum mechanics and the RDMs take over its role. However, various methods studied so far to determine the RDM without using the wave function [1] were successful only for limited systems, because of the  $N$ -representability problem [2]. Because the fermion's wave function is antisymmetric with respect to the permutation of particles (Pauli principle), physically acceptable RDM must satisfy some strong conditions (the  $N$ -representability conditions), which are not completely known except for 1-RDM [2].

The significance of our Hamiltonian is that it contains only one- and two-body operators. By using this special property, are there any methods to solve the quantum-mechanical problem more easily than by the traditional approach? It is clear that the Schrödinger equation does not use this property explicitly, because the Schrödinger equation is

also applicable to the system with three-body interaction.

Recently we and others developed a method which uses the two-body nature of the Hamiltonian explicitly to determine the RDM of general systems [3–5]. We solved the equation called the “hierarchy,” “density,” or “contracted Schrödinger” equation [6,7],

$$R^{(n)} = 0. \quad (1.1)$$

The  $n$ th-order energy density matrix ( $n$ -EDM) is given by

$$\begin{aligned} R^{(n)} = & -E\Gamma^{(n)} + \left\{ \sum_i^n v(r'_i) + \sum_{i>j}^n w(r'_i, r'_j) \right\} \Gamma^{(n)} \\ & + \binom{n+1}{1} \int \left\{ v(r_{n+1}) + \sum_i^n w(r'_i, r_{n+1}) \right\} \\ & \times \Gamma^{(n+1)} dr_{n+1} + \binom{n+2}{2} \\ & \times \int w(r_{n+1}, r_{n+2}) \Gamma^{(n+2)} dr_{n+1} dr_{n+2}, \quad (1.2) \end{aligned}$$

where  $\binom{n}{k}$  is the binomial coefficient. In the domain of the physically acceptable RDMs, Eq. (1.1) with  $n \geq 2$  is equiva-

lent to the Schrödinger equation, and only the exact RDMs of the ground or excited states satisfy it [7].

This equivalence shows that the  $N$ -representable 4-RDM uniquely determines the nondegenerate wave function. This one-to-one mapping is true for both the ground and the excited states, in contrast to the Hohenberg-Kohn theorem [8,9]. Our new method uses the density matrix as the basic variable and the density equation to determine it, instead of the wave function and the Schrödinger equation.

The equilibrium state of the finite-temperature system with a fixed number of particles was represented by the statistical operator  $\hat{\rho} = \sum_i |\Psi_i\rangle\langle\Psi_i| e^{-\beta E_i} / Z$ , where  $E_i$ ,  $|\Psi_i\rangle$ , and  $Z$  are the energy, wave function, and the partition function, respectively. All the thermodynamic quantities and the expectation values of the operators can be calculated from the partition function and the 2-RDM. Using the two-body nature of the Hamiltonian, it is possible to determine these quantities without calculating the wave function or 2-RDM of each eigenstate. In Sec. II we present the equation to determine the partition function and the 2-RDM directly, which can be seen as the extension of the density equation to the finite-temperature systems.

Since the second-order density equation, which is the lowest-order equation equivalent to the Schrödinger equation, also depends on the 3- and 4-RDMs, it is indeterminate without additional constraint, that is, the  $N$ -representability conditions. Under the current knowledge of the  $N$ -representability conditions, the density equation imposing known  $N$ -representability conditions may have highly degenerate nonphysical solutions and probably does not yield the isolated exact solution [10]. Hence we and others adopted the functional approach expressing the  $(n+1)$ - and the  $(n+2)$ -RDMs in terms of the  $n$ -RDM to remove the indeterminacy. The existence of such functionals is discussed in Sec. II. The approximate functional also functions as the  $N$ -representability conditions:  $N$ -representability is one of the properties to be approximated.

Various approximate functionals to express the higher-order RDMs were reported [4,5,11], and with these functionals, the second-order density equation was solved for atoms, molecules [3,4], and a model system [5]. These results were very promising, giving energies and RDMs as accurate as, or more accurate than the SDCI (single and double excitation configuration interaction) method, exactly  $N$ -representable 1-RDMs, and the 2-RDMs almost satisfied some important  $N$ -representability conditions. The density-equation method offers an entirely new alternative in quantum mechanics.

Our approximate functionals based on the perturbation theory yield the 3- and 4-RDMs of the exact eigenstate from the corresponding 2-RDM for a weakly perturbed system. Thus the same method may also be applicable to the excited states. In this paper we reported the determination of the excited-state 2-RDMs by the density-equation method with these functionals. From a different point of view, Mazziotti expressed the 4-RDM with several parameters and solved the density equation for the excited states of the quasispin model [5].

In the functional approach, the quality of the approximate functional determines the quality of the solution. Based on Green's-function (GF) theory, we developed the approximate functionals for higher-order RDMs, whose accuracy is up to

the second-order of the electron correlations. This approximation gave quantitative results for singly bonded molecules, but the errors of the multiply bonded molecules are larger, showing the importance of the higher-order terms. No other density-equation results were reported for these molecules.

In addition to the quantitative feature, higher-order perturbation terms have significant effects in many systems. For example, in the uniform electron gas or interacting hard spheres, simple perturbation expansion diverges, and the resummation of the infinite series of the physically important GF diagrams is necessary. Although the density-equation method may sum up some infinite series through the iterative calculation of the 2-RDM, the use of the more accurate, higher-order approximation is indispensable in solving the general systems including metals and semiconductors. Since the summation of the physically important RDM diagrams by the previous method [4] is difficult, we develop a diagrammatic method of EDM to sum up the Parquet diagram including the infinite series of ladder and bubble diagrams.

In large systems, explicit construction of the  $(n+1)$ - and  $(n+2)$ -RDMs requires much computational time, and the direct calculation of the energy density matrix without constructing the  $(n+1)$ - and  $(n+2)$ -RDMs is desirable. Our new method yields the second-order energy density matrix directly without explicitly constructing the 3- and 4-RDMs. Development of the direct calculation method of 2-EDM will be a first step in applying the density-equation method to large systems.

The organization of this paper is as follows. In Sec. II, we review the theoretical foundations to reconstruct the higher-order RDMs. The equation for the direct determination of the density matrix of the finite-temperature canonical ensemble is presented. In Sec. III we reformulate our previous approximation for higher-order RDMs in terms of the lower-order ones [4], and the accuracy of the various reconstruction functionals for the excited states is examined. In Sec. IV we examine the general structure of the energy density matrix using the generating functionals. In Sec. V we present the integral equations to sum up the Parquet diagrams of the second-order energy density matrix. In Sec. VI we apply this new approximation for the ground states and the closed-shell excited states of atoms and molecules and compare the results with the previous approximation and the wave-function methods.

## II. FORMAL THEOREM

In this section we first review the fundamental question in the density-equation approach: what order RDM has enough information to uniquely determine the wave function.

The RDM is said to be pure-state  $N$ -representable if the RDM is derivable from an antisymmetric function of  $N$  particles, and ensemble  $N$  representable if it is derivable from a mixed state with  $N$  particles.

We will review the theorems about the ground state first. The Hohenberg-Kohn theorem [8] demonstrates that the ground-state electron density is sufficient to determine the external potential of the Hamiltonian. Mazziotti pointed out [5] that the electron density alone cannot determine the wave function without the knowledge of the kinetic and the Cou-

lomb repulsion terms. By using the variational principle of the ground-state energy, Rosina proved that the  $N$ -representable 2-RDM of the ground state has enough information to determine the two-body Hamiltonian [12]. We can conclude that it is in principle possible to reconstruct the wave function and hence the higher-order RDMs of the ground state of the two-body Hamiltonian in terms of the 2-RDM.

Next we consider the excited states. It is easy to show that the 4-RDM of the nondegenerate state of the two-body Hamiltonian has enough information to determine the wave function. This is a consequence of MacDonald's variational principle: each eigenstate corresponds to the minimum of the expectation value of a four-body operator,  $\langle (H-E)^2 \rangle$ . Hence the 4-RDM of the nondegenerate state of the two-body Hamiltonian has a unique preimage in the set of ensemble  $N$ -representable density matrices. It can also be proved that these 4-RDMs are the extreme elements of the convex set of the 4-RDMs.

If we restrict the two-body interaction in the Hamiltonian as the Coulomb interaction, two different wave functions  $|\Psi\rangle$  and  $|\Psi'\rangle$ , which are the nondegenerate eigenfunctions of Hamiltonians  $H=v+w$  and  $H'=v'+w$ , do not yield the same  $\Gamma^{(3)}$ . Assuming that  $|\Psi\rangle$  and  $|\Psi'\rangle$  yield the same  $\Gamma^{(3)}$ , using MacDonald's variational principle,

$$\langle \Psi' | (H-E)^2 | \Psi' \rangle + \langle \Psi | (H'-E')^2 | \Psi \rangle > 0. \quad (2.1)$$

On the other hand, the same formula becomes

$$\begin{aligned} & \langle \Psi' | (H-E)^2 - (H'-E')^2 | \Psi' \rangle \\ & + \langle \Psi | (H'-E')^2 - (H-E)^2 | \Psi \rangle = 0 \end{aligned}$$

because  $|\Psi\rangle$  and  $|\Psi'\rangle$  yield the same  $\Gamma^{(3)}$  and  $(H-E)^2 - (H'-E')^2$  is a three-body operator. This contradiction indicates that the  $N$ -representable  $\Gamma^{(3)}$  has enough information to determine the wave function among all the nondegenerate eigenfunctions of the Hamiltonians with fixed two-body interaction.

Recently without using the variational principle, Mazzotti proved the following theorem [5]: if each state of the two-body Hamiltonian may be distinguished from other states by at least one two-body operator, then the 2-RDM has a unique preimage in the set of pure-state  $N$ -representable density matrices. A corollary of this theorem is that the  $p$ -RDMs of each state are the unique functionals of the 2-RDM. Based on this theorem he proposed a new reconstruction method called ensemble representable method, and calculated the 2-RDMs of the excited states of the quasi-spin model by solving the density equation.

The density equation for the eigenstate is extended to the finite-temperature, canonical ensemble with a fixed number of  $N$  particles. The necessary and sufficient condition for the  $n$ -RDM to be derivable from the statistical operator  $\hat{\rho} = e^{\beta(F-H)}$  is to satisfy the equation

$$\begin{aligned} & -\frac{\partial}{\partial \beta} \Gamma^{(n)}(r'_1, \dots, r'_n | r_1, \dots, r_n) \\ & = R^{(n)}(r'_1, \dots, r'_n | r_1, \dots, r_n) \\ & = \frac{1}{n!} \text{Tr} \{ \phi^\dagger(r_1) \cdots \phi^\dagger(r_n) \phi(r'_1) \cdots \phi(r'_n) (H-E) \hat{\rho} \}, \end{aligned} \quad (2.2)$$

where  $\beta$  is the inverse temperature,  $F$  is the Helmholtz free energy  $F = -\beta^{-1} \log \text{Tr} \exp(-\beta H)$ , and  $E$  is the expectation value of  $H$ .  $\text{Tr}$  indicates the sum of the diagonal elements in the  $N$ -particle Hilbert space. The right-hand side (rhs) of Eq. (2.2) is written with the  $n$ -,  $(n+1)$ -, and  $(n+2)$ -RDMs, as shown in Eq. (1.2). The necessity for the theorem is trivial if we notice that the true statistical operator satisfies the equation

$$(\partial_\beta + H - E) \hat{\rho} = 0.$$

$\partial_\beta$  is an abbreviation for  $\partial/\partial\beta$ . We will prove the sufficiency for the second-order equation, because if the higher-order equation is satisfied, the lower order is also satisfied. Suppose that the ensemble representable statistical operator  $\hat{\rho}'$  yields the  $n$ -,  $(n+1)$ -, and  $(n+2)$ -RDMs which satisfy Eq. (2.2). Then it follows

$$-\partial_\beta \text{Tr} \{ (\partial_\beta + H - E) \hat{\rho}' \} + \text{Tr} \{ (H - E) (\partial_\beta + H - E) \hat{\rho}' \} = 0,$$

and hence

$$\begin{aligned} & \int_0^{+\infty} \text{Tr} \{ (-\partial_\beta + H - E) (\partial_\beta + H - E) \hat{\rho}' \} d\beta \\ & = \int_0^{+\infty} \sum_k |(\partial_\beta + H - E) |k(\beta)\rangle|^2 d\beta = 0. \end{aligned}$$

We write the  $N$ -particle sector of  $\hat{\rho}'$  as  $\sum_k |k(\beta)\rangle \langle k(\beta)|$ . The above equation indicates that  $\hat{\rho}'$  satisfies the same equation as  $\hat{\rho}$ , and both are equivalent in the  $N$ -particle Hilbert space and yield the same exact RDMs. Other thermodynamic quantities including the partition function can be calculated from the energy expectation value  $E(\beta)$ .

Equation (2.2) is completely different from the equation of motion of the thermal Green's function [13] and the equation of quantum Bogolyubov-Born-Green-Kirkwood-Yvon (BBGKY) hierarchy recently reported [14]. These equations establish the relationship between  $n$ - and  $(n+1)$ -RDMs, while Eq. (2.2) describes the relationship among  $n$ -,  $(n+1)$ -, and  $(n+2)$ -RDMs. The anti-Hermite part of Eq. (2.2) is equivalent to the BBGKY hierarchy equation and the equation of motion of the thermal Green's function at the zero time interval.

Similar to the 2-RDM of the ground state, the 2-RDM of the finite-temperature canonical ensemble has enough information to determine  $H$ , and we can use the 2-RDM to represent the state. There are no two-body Hamiltonians  $H \neq H'$  which yield the same 2-RDM of the finite-temperature systems. It is a consequence of the variational principle of the Helmholtz free energy [9]. Hence the reconstruction of the higher-order RDMs in terms of the 2-RDM is in principle

possible, and the decoupling method based on the thermal Green's function provides a systematic way toward the exact solution. The use of Eq. (2.2) together with the reconstruction functionals offers a new alternative to the traditional approach for the finite-temperature systems. The simplest approximation of  $n$ -RDM in terms of 1-RDM by Löwdin's formula together with the first-order equation of Eq. (2.2) yields the Fermi distribution function for a noninteracting system. The proof is given in Appendix A. We will report the finite-temperature results using a more accurate approximation and the second-order equation in a future paper.

### III. APPROXIMATIONS OF HIGHER-ORDER RDMs

In this section we summarize the approximations reported so far, and the accuracy of our approximation for the excited states is examined. In the previous papers [4], we used the Green's-function (GF) method to derive the relationships among the higher-order RDMs and the lower-order ones. The  $n$ -RDMs and  $n$ -particle many-body GFs ( $n$ -GFs) are defined as [9,13]

$$\begin{aligned} \Gamma^{(n)}(r'_1, \dots, r'_n | r_1, \dots, r_n) \\ = \frac{1}{n!} \langle \phi^\dagger(r_1), \dots, \phi^\dagger(r_n) \phi(r'_1), \dots, \phi(r'_n) \rangle \end{aligned}$$

$$\begin{aligned} i^n G^{(n)}(x'_1, \dots, x'_n | x_1, \dots, x_n) \\ = \langle T[\phi(x'_1), \dots, \phi(x'_n) \phi^\dagger(x_n), \dots, \phi^\dagger(x_1)] \rangle, \end{aligned}$$

where  $r_i$  denotes the set of position and spin coordinates,  $x_i$  denotes the set of time, position and spin coordinates, of the  $i$ th electron,  $\phi^\dagger$  and  $\phi$  denote the creation and annihilation field operators in the Heisenberg representation, and  $T$  denotes the time-ordering operator. We define the time ordering of the operators at equal times as the normal order: creation operators are ordered to the left of the annihilation operators, multiplied by the signum of the permutation. We will suppress the time variable when it equals zero. The RDMs are expressed with the GFs as

$$\begin{aligned} \Gamma^{(n)}(r'_1, \dots, r'_n | r_1, \dots, r_n) \\ = \frac{(-i)^n}{n!} G^{(n)}(r'_1, \dots, r'_n | r_1, \dots, r_n). \end{aligned} \quad (3.1)$$

Many-particle GFs are represented with Feynman's diagrams [13]. For example,  $G^{(2)}$  is expressed as

$$G^{(2)} = \left| \right| - \text{X} + \text{W} - \text{X} \quad (3.2)$$

The bold line denotes the exact one-particle GF, while the wavy line denotes the exact two-body vertex  $V$  [13]. Each  $G^{(n)}$  diagram has a coefficient of  $i^{2l+m-k-n}$ , where  $l$  is the number of the closed  $G^{(1)}$  loops,  $m$  is the number of the unperturbed  $G^{(1)}$  lines, and  $k$  is the order of the perturbation.

Since RDMs are a special case of GFs with time variables equal to zero, the same Feynman diagrams represent RDMs.

$$2!\Gamma^{(2)} = \left| \right| - \text{X} + \text{W} - \text{X} \quad (3.3a)$$

$$3!\Gamma^{(3)} = \left| \right| \left| \right| + \text{W} \left| \right| + \left| \right| \text{W} \dots \quad (3.3b)$$

$$4!\Gamma^{(4)} = \left| \right| \left| \right| \left| \right| + \text{W} \left| \right| \left| \right| + \left| \right| \text{W} \left| \right| \left| \right| + \left| \right| \left| \right| \text{W} \left| \right| + \left| \right| \left| \right| \left| \right| \text{W} \dots \quad (3.3c)$$

In Eqs. (3.3b) and (3.3c) typical diagrams are shown. Since the time variables of the external lines are zero, the isolated bold line represents the exact  $\Gamma^{(1)}$ . We define the vertex part of 2-RDM,  $V_\Gamma$ , as the third term of Eq. (3.3a).

Several methods are reported to derive the relationship among RDMs. In the previous paper we derived the relations by comparing the Feynman diagrams of  $n$ -RDM with those of  $k$ -RDMs of  $k < n$ . By using the new generating functionals of RDMs, which do not involve the time variables, Mazziotti reported a more concise method [5] to derive the relationships among  $n$ -RDMs with  $n \leq 6$ . Generating functionals are also known to be useful to analyze the structure of the many-particle GF [13]. In Secs. III and IV we use these techniques. We denote the connected piece of  $n$ -GF as  $G_c^{(n)}$  which cannot be expressed as a simple product of lower-order GFs.  $\Gamma_c^{(n)}$  is defined similarly, which correspond to the last terms in Eqs. (3.3b) and (3.3c). By definition, functionals  $Z_G[J]$  and  $W_G[J]$  generate  $G^{(n)}$  and  $G_c^{(n)}$  as well as  $\Gamma^{(n)}$  and  $\Gamma_c^{(n)}$ . For example,

$$\begin{aligned} \Gamma^{(n)}(r'_1, \dots, r'_n | r_1, \dots, r_n) \\ = \lim_{J \rightarrow 0} \frac{(-1)^n}{n!} \frac{\delta^{2n} Z_G}{\delta J^*(r'_1) \dots \delta J^*(r'_n) \delta J(r_n) \dots \delta J(r_1)} \end{aligned}$$

in which  $J$  and  $J^*$  are the Grassmann variables [5,13]. Instead of using Mazziotti's generating functional of RDMs, we use the generating functional of GFs,

$$Z_G = \langle \Psi | T[e^{-iS_1}] | \Psi \rangle, \quad (3.4)$$

$$S_1 = \int \{J^*(x) \phi(x) + \phi^\dagger(x) J(x)\} dx,$$

to emphasize the similarity between GF and RDM, and to use the diagrammatic analysis.

By differentiating the relation between  $Z_G$  and  $W_G$ ,

$$Z_G = \exp W_G, \quad (3.5)$$

and taking the limit  $J \rightarrow 0$ , the relation among GFs [13] or RDMs [5] is obtained:  $\Gamma^{(n)}$  is expressed with  $\Gamma_c^{(n)}$  and the products of the  $\Gamma_c^{(k)}$  with  $k < n$ . The same result is obtained by comparing the Feynman diagrams. This relation among RDMs is useful not only to analyze the structure of the RDMs but also to approximate the higher-order RDMs. For example, the approximation of Valdemoro and co-workers can be derived by neglecting some connected pieces.

In the previous paper we used the same approximation for the unconnected 3- and 4-RDMs, and also approximated the connected piece of 3-RDM as follows. Exact  $G^{(1)}$  satisfies an approximate relation when  $tt' < 0$ ,

$$\begin{aligned} iG^{(1)}(x', x) &\approx \int dq dq' G_0^{(1)}(x', q) P_0(q, q') G^{(1)}(q', x) \\ &\approx \int dq dq' G^{(1)}(x', q) P(q, q') G^{(1)}(q', x), \end{aligned} \quad (3.6)$$

$$\begin{aligned} P(q, q') &= P_0(q, q') - \int P(q, r') \gamma(r', r) P_0(r, q') dr dr', \\ P_0(q, q') &= 2\Gamma_0^{(1)}(q, q') - \delta(q - q'), \\ \gamma(q, q') &= \Gamma^{(1)}(q, q') - \Gamma_0^{(1)}(q, q'), \end{aligned} \quad (3.7)$$

in which  $r$  and  $q$  denote the set of position and spin coordinates, while  $x$  denotes the set of time, position, and spin coordinates. Unperturbed  $G^{(1)}$  satisfies Eq. (3.6) when  $P = P_0$ . It is a consequence of the rules of subsequent events in the path-integral theory [15]. Equation (3.7), which looks like Dyson's equation, determines  $P$ . We used the approximate relationship of Eq. (3.6) to express the connected 3-RDM, the last term in Eq. (3.3b), in terms of 1- and 2-RDMs. We replaced  $G^{(1)}$  joining two vertices in the  $\Gamma_c^{(3)}$  with the rhs of Eq. (3.6). The vertex diagram with four external legs was next replaced with  $V_\Gamma$ ,

$$\begin{aligned} V_\Gamma(r'_1, r'_2 | r_1, r_2) &= -i \int dx_1 \dots dx_2 V(x'_1, x'_2 | x_1, x_2) \\ &\quad \times G^{(1)}(r'_1 | x'_1) G^{(1)}(r'_2 | x'_2) \\ &\quad \times G^{(1)}(x_1 | r_1) G^{(1)}(x_2 | r_2), \end{aligned} \quad (3.8)$$

which was calculated from the given 1- and 2-RDMs by Eq. (3.3a). The final formula for the connected 3-RDM,

$$\begin{aligned} \Gamma_c^{(3)} &= \frac{1}{3!} \int V_\Gamma(r'_1, r'_2 | q, r_3) P(q, q') \\ &\quad \times V_\Gamma(q', r'_2 | r_1, r_2) dq dq' + \dots, \end{aligned} \quad (3.9)$$

contains no time integration, in contrast to the GF theory. The relationships among the spinless  $n$ -RDMs  ${}^n D$  are obtained by summing up the spin variables [4].

Without using the time-dependent theory, Eq. (3.9) could be understood in a different way. Suppose we keep the first-order perturbation terms of the wave function in the cluster expansion form,

$$\begin{aligned} |\Psi\rangle &= N \exp(\hat{T}_1 + \hat{T}_2 + \dots) |\text{HF}\rangle \\ \hat{T}_n &= T^{(n)}_{j_1 \dots j_n} a_{j_1}^\dagger \dots a_{j_n}^\dagger a_{j_n} \dots a_{j_1} \end{aligned}$$

in which  $T^{(n)}$  denotes the  $n$ -body cluster amplitude and  $|\text{HF}\rangle$  denotes the Hartree-Fock Slater determinant. Under this approximation the only nonzero elements in the cluster amplitude is  $T^{(2)ilj_2}$ , where  $j_k$  belongs to the occupied orbitals and

$i_k$  belongs to the virtual orbitals, and other cluster amplitudes  $T^{(n)}$  ( $n \neq 2$ ) can be neglected [16]. Then the connected piece of 2-RDM is given by the formula

$$\begin{aligned} \Gamma_c^{(2)ilj_2} &= \frac{1}{2} \{ \langle \text{HF} | a_{i_1}^\dagger a_{i_2}^\dagger a_{j_2} a_{j_1} \hat{T}_2 | \text{HF} \rangle \\ &\quad + \langle \text{HF} | \hat{T}_2^\dagger a_{i_1}^\dagger a_{i_2}^\dagger a_{j_2} a_{j_1} | \text{HF} \rangle \}. \end{aligned}$$

As is seen, this  $\Gamma_c^{(2)}$  completely determines the nonzero elements of the first-order perturbation terms of  $T^{(2)}$ . Once we get the cluster amplitude, we can calculate the leading term of the  $\Gamma_c^{(3)}$  which is the second order. By using this first-order  $T^{(2)}$  the only nonzero elements are

$$\Gamma_c^{(3)il_1i_2i_3} = \frac{1}{3!} \langle \text{HF} | \hat{T}_2^\dagger a_{i_1}^\dagger a_{i_2}^\dagger a_{i_3}^\dagger a_{j_3} a_{j_2} a_{j_1} \hat{T}_2 | \text{HF} \rangle.$$

Substituting the amplitude with  $\Gamma_c^{(2)}$  and evaluating the expectation values of the creation and annihilation operators, we get the leading term of Eq. (3.9).

We then compare the various approximations reported to date. Valdemoro and co-workers included explicitly the first two terms of Eq. (3.3b) for 3-RDM and the first three terms of Eq. (3.3c) for 4-RDM [3]. This approximation includes zeroth- and first-order perturbation terms in electron correlations in both 3- and 4-RDMs, provided that the 3- and 4-RDMs are constructed from the 1- and 2-RDMs. They took into account the connected piece of 3-RDM by correcting the approximated 3-RDM with some  $N$ -representability conditions, or by contracting the approximate 4-RDM to the 3-RDM. Their approximation together with the second-order density equation gave good results for the four-electron atom and ions, and the six-electron molecule of  $\text{BeH}_2$ .

In the previous papers [4], we explicitly included the first three terms of Eq. (3.3b) for 3-RDM and the first four terms of Eq. (3.3c) for 4-RDM. This approximation includes the terms up to the second-order perturbation of the electron correlations for both 3- and 4-RDMs and omits some of the third- and the higher-order perturbation terms. The fourth term of Eq. (3.3c) for 4-RDM represents the simultaneous collisions of two electron pairs. The density-equation method with this decoupling approximation gave better results than the SDCI method for closed-shell atoms and molecules. The second-order perturbation terms are essential for the correct description of electron correlations in atoms and molecules.

Based on these studies, Mazziotti proposed a new approximation scheme for 3-RDM [5]. He contracted the approximated 4-RDM functional to the 3-RDM to generate a system of equations for the 3-RDM. This system of equations yields the 3-RDM which is correct through second order. His approximation works well for the quasispin model, giving better results than the SDCI method.

It is interesting to examine whether the density-equation method with approximate functional can be applied to the excited states. We examine the accuracy of the functionals for the excited states. We approximated the 3-RDM using the first- and second-order functionals, from the exact 1- and 2-RDMs of the ground and five singlet excited states of the

TABLE I. Errors of the approximated RDMs calculated by the various approximate functionals for the ground and excited states of Be atom.  $\Gamma_0(2200)$  indicates the electron occupation in the unperturbed 1-RDM used in Eq. (3.7). Numbers in square brackets indicate powers of 10.

	Ground			Excited states		
Energy	-14.582 69	-13.202 01	-11.762 86	-9.198 39	-8.206 16	-3.056 01
Main config. <sup>a</sup>	1.00(2200)	0.71(2110)	1.00(2020)	0.70(1210)	0.70(1120)	0.99(0220)
		+0.71(2110)		+0.70(1210)	+0.70(1120)	
Method	Errors of the approximated 3-RDM <sup>b</sup>					
1st order	1.755[-3]	6.257[-2]	1.025[-3]	5.989[-2]	5.822[-2]	8.517[-4]
2nd order						
$\Gamma_0(2200)$	2.719[-4]	1.462	5.552[-3]	1.465	1.442	1.558[-3]
$\Gamma_0(2020)$	2.800[-3]	4.900[-1]	5.700[-3]	1.092	1.095	1.138[-1]
$\Gamma_0(0220)$	2.799[-3]	1.106	2.279[-1]	5.026[-1]	1.059	3.808[-4]
	Errors of the approximated 4-RDM <sup>b</sup>					
1st order	7.601[-4]	4.705[-2]	5.102[-4]	4.565[-2]	4.604[-2]	3.307[-4]
2nd order	3.279[-5]	2.573[-1]	1.787[-5]	2.580[-1]	2.589[-1]	9.094[-6]
3rd order						
$\Gamma_0(2200)$	1.321[-5]	1.291	4.500[-4]	1.294	1.300	1.755[-4]
$\Gamma_0(2020)$	3.231[-5]	3.716[-1]	1.651[-5]	8.258[-1]	8.316[-1]	1.187[-2]
$\Gamma_0(0220)$	2.887[-5]	8.412[-1]	5.144[-1]	3.783[-1]	7.960[-1]	6.815[-6]

<sup>a</sup>CI coefficient and electron occupations in the four Hartree-Fock orbitals.

<sup>b</sup>Errors of the RDMs measured by the Euclidean norm.

Be atom. The errors of the approximated 3-RDMs are measured by the Euclidean norm. Similarly the 4-RDMs are approximated with the first-, second-, and third-order functionals from the exact 1-, 2-, and 3-RDMs, and the errors of the 4-RDMs are calculated. The results are summarized in Table I. Because the second-order functionals of the 3-RDM and the third-order functionals of the 4-RDM contain the unperturbed 1-RDM, we used three different  $\Gamma_0^{(1)}$  in Eq. (3.7). In Table I,  $\Gamma_0(2020)$  indicates that the four electrons occupy the first and the third Hartree-Fock orbitals in the unperturbed 1-RDM. The main configurations in each excited state are shown in Table I. The second and the fifth excited states are closed-shell, two-electron excited states, while the first, third, and the fourth excited states are the open-shell excited states.

As shown in Table I, the errors of the approximated 3-RDMs by the first-order functional are about  $10^{-3}$  for the closed-shell states and about  $10^{-2}$  for the open-shell states. The first-order functional contains the first and the second terms of Eq. (3.3b). The effect of the second-order perturbation term, which is the third term of Eq. (3.3b), strongly depends on the nature of the excited states and also on the unperturbed 1-RDM used in Eq. (3.7). In the open-shell states, the second-order correction goes in the wrong direction and the errors become as large as 1. In the closed-shell states, the second-order correction reduces the errors of 3-RDMs by an order of magnitude, provided that the unperturbed 1-RDM is the proper approximate 1-RDM. The other choice of  $\Gamma_0^{(1)}$  gives errors almost the same as, or slightly greater than, those of the first-order approximation.

A similar tendency is observed for 4-RDM. The errors of the first-order approximation are about  $10^{-4}$  for the closed-shell states, while they are about  $10^{-2}$  for the open-shell states. The errors of the first-order functional in the open-shell states are slightly greater than those in the closed-shell

states. The fourth term of Eq. (3.3c), which is the second order of the electron correlation, improves the 4-RDM by an order of magnitude for the closed-shell states. On the other hand, the same correction goes in the wrong direction in the open-shell states, although this correction does not use the unperturbed 1-RDM. The third-order perturbation term, which is the last term of Eq. (3.3c), works well for the closed-shell states, if the proper unperturbed 1-RDM is used. Another choice of  $\Gamma_0^{(1)}$  does not improve the 4-RDMs. We conclude that if the proper unperturbed 1-RDM is used, the 3- and 4-RDMs of the closed-shell state are accurately approximated by the second- or third-order functionals. This unperturbed 1-RDM selects the closed-shell states to be approximated.

Our functionals based on Green's-function theory can accurately approximate the closed-shell RDMs of the ground and excited states. However, the approximation of the open-shell RDMs needs other new functionals. The accuracy of the approximated RDMs of the closed-shell state depends on the order of the perturbation of the functionals and the strength of the electron correlations. Although our previous second-order approximation gave satisfactory results for singly bonded molecules, the errors of the multiply bonded molecules are greater. The effects of the higher-order perturbation terms are not negligible for these molecules. In addition to this quantitative feature, there are many systems in which the higher-order perturbation terms have significant effects, for example, the uniform electron gas and the interacting hard spheres. In these systems, simple perturbation expansion may be useless because the bubble and ladder diagrams of any orders diverge. Summation of the physically important diagrams up to any orders is necessary. This is the reason why we develop the more accurate, higher-order approximations, even if the second-order approximation yields good results for atoms and molecules. The less accurate re-

sults of multiply bonded molecules are understood if we notice that the  $\pi$  electron is less bounded than the  $\sigma$  electron, and the higher-order ring diagrams become more important for these molecules. Since the approximation of higher-order RDMs also functions as the  $N$ -representability conditions, it is important to use a good approximation not only to obtain a good energy but also to ensure the representability of the calculated RDMs.

In the density-equation approach, we approximate the higher-order RDMs to calculate the EDM. Because the explicit construction of higher-order RDMs is very expensive, for example the calculation of the 4-RDM requires about  $M^8$  computational time, where  $M$  is the number of the basis functions, the direct calculation method of EDM without explicitly constructing the higher-order RDMs is desirable. In Secs. IV and V we explore a direct method which sums up the physically important diagrams of 3- and 4-RDMs, for example the ladder and bubble diagrams up to any orders. At the outset we analyze the general structure of the EDM by the generating functionals.

#### IV. GENERATING FUNCTIONAL OF THE ENERGY DENSITY MATRIX

In this section we define the generating functionals of the energy density matrix and the connected piece of EDM, derive the relationships between these two functionals, and reveal the structure of the higher-order EDMs. Since  $n$ -EDM is defined by Eq. (1.2) in terms of the  $n$ -,  $(n+1)$ -, and  $(n+2)$ -RDMs, the generating functional of EDM is

$$\begin{aligned} Z_E &= \langle \Psi | T[e^{-iS_1}] (H-E) | \Psi \rangle \\ &= \int \left\{ J^*(r) + \frac{\delta}{\delta J(r)} \right\} \frac{\delta Z_G}{\delta J^*(r')} v(r, r') dr dr' \\ &\quad + \frac{1}{2} \int \left\{ J^*(r) + \frac{\delta}{\delta J(r)} \right\} \left\{ J^*(r') + \frac{\delta}{\delta J(r')} \right\} \\ &\quad \times \frac{\delta^2 Z_G}{\delta J^*(r') \delta J^*(r)} w(r, r') dr dr' - EZ_G, \end{aligned} \quad (4.1)$$

where  $S_1$  is given by Eq. (3.4). The  $n$ -EDM is given as

$$\begin{aligned} R^{(n)}(r'_1, \dots, r'_n | r_1, \dots, r_n) \\ = \lim_{J \rightarrow 0} \frac{(-1)^n}{n!} \frac{\delta^{2n} Z_E}{\delta J^*(r'_1) \dots \delta J^*(r'_n) \delta J(r_n) \dots \delta J(r_1)}. \end{aligned} \quad (4.2)$$

The EDM and the generating functional  $Z_E$  are identically zero if  $|\Psi\rangle$  and  $E$  are the eigenfunction and the corresponding eigenvalue of  $H$ .

In the interaction representation the generating functional of GF is

$$Z_G = \frac{\langle \Phi | T[e^{-i(S_1+S_2)}] | \Phi \rangle}{\langle \Phi | T[e^{-iS_2}] | \Phi \rangle},$$

$$S_1 = \int \{ J^*(x) \phi_I(x) + \phi_I^\dagger(x) J(x) \} dx,$$

$$\begin{aligned} S_2 &= \int \phi_I^\dagger(x) \tilde{v}(x, x') \phi_I(x') dx dx' \\ &\quad + \frac{1}{2} \int \phi_I^\dagger(x) \phi_I^\dagger(x') w(x, x') \phi_I(x') \phi_I(x) dx dx', \end{aligned} \quad (4.3)$$

$$\tilde{v}(x, x') = \{ v(r, r') - h_0(r, r') \} \delta(t - t'),$$

$$w(x, x') = w(r, r') \delta(t - t'),$$

where  $\phi_I^\dagger$  and  $\phi_I$  are the creation and annihilation field operators in the interaction representation,  $h_0$  is an unperturbed Hamiltonian,  $\tilde{v}$  and  $w$  are the perturbation potentials, and  $|\Phi\rangle$  is the unperturbed state from which the exact eigenstate  $|\Psi\rangle$  evolves adiabatically.

Using Eq. (4.3), the higher-order derivative of  $Z_G$  with respect to  $J$  and  $J^*$  is expressed by the derivative with respect to  $\tilde{v}$  and  $w$ ,

$$\frac{\delta Z_G}{\delta \tilde{v}(x, x')} = i \frac{\delta^2 Z_G}{\delta J^*(x') \delta J(x)} + Z_G G^{(1)}(x' | x), \quad (4.4a)$$

$$\begin{aligned} -2 \frac{\delta Z_G}{\delta w(x, x')} &= i \frac{\delta^4 Z_G}{\delta J^*(x) \delta J^*(x') \delta J(x') \delta J(x)} \\ &\quad + i Z_G G^{(2)}(x, x' | x, x'). \end{aligned} \quad (4.4b)$$

Using Eqs. (3.5), (4.1), and (4.4), the generating functional of EDM is

$$Z_E = W_E \exp W_G, \quad (4.5)$$

where  $W_E$  is given by

$$W_E = W_{E1} + W_{E2} + W_{E3} + W_{E4} + W_{E5},$$

$$W_{E1} = \int J^*(r) \frac{\delta W_G}{\delta J^*(r')} v(r, r') dr dr', \quad (4.6a)$$

$$W_{E2} = i \int \frac{\delta W_G}{\delta \tilde{v}(x, x')} v(r, r') \delta(t) \delta(t') dx dx', \quad (4.6b)$$

$$\begin{aligned} W_{E3} &= \frac{1}{2} \int J^*(r) J^*(r') \left\{ \frac{\delta W_G}{\delta J^*(r')} + \frac{\delta}{\delta J^*(r')} \right\} \\ &\quad \times \frac{\delta W_G}{\delta J^*(r)} w(r, r') dr dr', \end{aligned} \quad (4.6c)$$

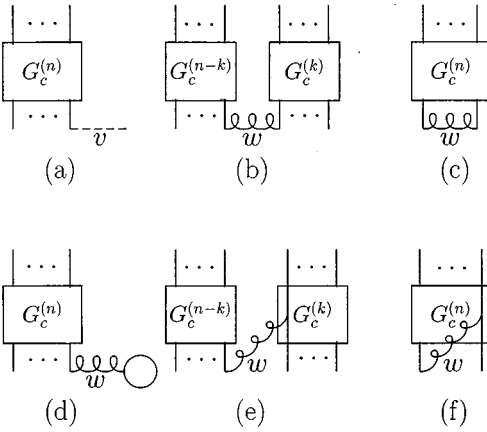


FIG. 1. Typical diagrams of the energy density matrix generated by Eqs. (4.6). The dotted line indicates the one-body potential of  $v$ , while the curly line indicates the Coulomb interaction of  $w$ .

$$W_{E4} = i \int J^*(r) \left\{ \frac{\delta W_G}{\delta \tilde{v}(x', x')} - i\rho(r') + \frac{\delta}{\delta \tilde{v}(x', x')} \right\} \\ \times \frac{\delta W_G}{\delta J^*(r)} w(r, r') \delta(t') dr dx', \quad (4.6d)$$

$$W_{E5} = i \int \frac{\delta W_G}{\delta w(x, x')} w(r, r') \delta(t) \delta(t') dx dx'. \quad (4.6e)$$

Equation (4.6b) shows that one perturbation potential  $\tilde{v}(x, x') = v(r, r') \delta(t-t')$  in  $W_G$  is replaced with  $v(r, r') \delta(t) \delta(t')$  in  $W_{E2}$ , while Eq. (4.6e) shows that one interaction line  $w(x, x') = w(r, r') \delta(t-t')$  in  $W_G$  is replaced with  $w(r, r') \delta(t) \delta(t')$  in  $W_{E5}$ . Hence  $W_{E2}$  generates the same Feynman diagrams as  $G_c^{(n)}$ , except that one perturbation potential  $\tilde{v}(x, x')$  is replaced with  $v(r, r') \delta(t) \delta(t')$ , and  $W_{E5}$  generates the same Feynman diagrams as  $G_c^{(n)}$ , except that one interaction line  $w(x, x')$  is replaced with  $w(r, r') \delta(t) \delta(t')$ . These generated diagrams of  $R_c^{(n)}$  are almost the same as those of  $G_c^{(n)}$ .

In Eq. (4.1) only the creation and annihilation operators in the Hamiltonian are the Schrödinger representation, that is, the Heisenberg representation with  $t=0$ . Unfamiliar factors of  $\delta(t) \delta(t')$  and  $\delta(t')$  in Eq. (4.6) make the time variables of these operators zero.

Figure 1 shows the  $n$ -EDM diagrams generated by  $W_{E1}$ ,  $W_{E3}$ , and  $W_{E4}$ . Applying  $v(r, r')$  to the incoming legs of  $G_c^{(n)}$  gives the  $R_c^{(n)}$  shown in Fig. 1(a) generated by  $W_{E1}$ . Functional  $W_{E3}$  generates two kinds of diagrams: In Fig. 1(b) the incoming legs of  $G_c^{(n-k)}$  and  $G_c^{(k)}$  with  $k < n$  are joined with  $w$ . In Fig. 1(c), two incoming legs of  $G_c^{(n)}$  are joined with  $w$ . Functional  $W_{E4}$  generates three kinds of diagrams of Figs. 1(d)–1(f). Applying the Coulomb potential to the incoming legs of  $G_c^{(n)}$  gives the diagram of Fig. 1(d). In Fig. 1(e), an incoming leg of  $G_c^{(n-k)}$  is connected to an internal line of  $G_c^{(k)}$  with  $w$ , and in Fig. 1(f), an incoming leg is connected to an internal line of  $G_c^{(n)}$  with  $w$ .

Since  $W_G$  is the generating functional of connected GFs,  $n$ -EDM generated by  $W_E$ ,

$$R_c^{(n)}(r'_1, \dots, r'_n | r_1, \dots, r_n) \\ = \lim_{J \rightarrow 0} \frac{(-1)^n}{n!} \frac{\delta^{2n} W_E}{\delta J^*(r'_1) \dots \delta J^*(r'_n) \delta J(r_n) \dots \delta J(r_1)}, \quad (4.7)$$

is also the connected piece which cannot be written as a product of other connected pieces.

Equation (4.5) shows the relationship between the generating functional of EDM and that of connected EDM, which is useful in examining the structure of the EDMs. By differentiating it with respect to  $J$  and setting  $J=0$ , higher-order  $n$ -EDM  $R_c^{(n)}$  is expressed with the connected  $n$ -EDM  $R_c^{(n)}$  and the wedge product of  $R_c^{(k)}$  and  $\Gamma^{(n-k)}$  with  $k < n$ ,

$$R_c^{(n)}(r'_1, \dots, r'_n | r_1, \dots, r_n) \\ = \lim_{J \rightarrow 0} \frac{(-1)^n}{n!} \frac{\delta^{2n} (W_E Z_G)}{\delta J^*(r'_1) \dots \delta J^*(r'_n) \delta J(r_n) \dots \delta J(r_1)} \\ = \sum_{k=0}^n \binom{n}{k} R_c^{(k)} \wedge \Gamma^{(n-k)}. \quad (4.8)$$

We use the conventions of  $\Gamma^{(0)} = 1$  and  $R_c^{(0)} = 0$ . The wedge product is defined as [5]

$$R_c^{(k)} \wedge \Gamma^{(n-k)} = \left( \frac{1}{n!} \right)^2 \sum_{\pi, \pi'} \epsilon(\pi) \epsilon(\pi') \pi \pi' \\ \times R_c^{(k)}(r'_1, \dots, r'_k | r_1, \dots, r_k) \\ \times \Gamma^{(n-k)}(r'_{k+1}, \dots, r'_n | r_{k+1}, \dots, r_n)$$

in which  $\pi$  and  $\pi'$  permute the coordinates  $r_i$  and  $r'_i$  in all the possible  $(n!)$  manners, respectively, and  $\epsilon(\pi)$  is the signum of the permutation  $\pi$ . Equation (4.8) is easily verified by comparing the number of the terms on each side, or by calculating the lower-order derivatives. For example, using  $R_c^{(1)} = R^{(1)}$ ,  $R_c^{(2)}$  is expressed as

$$R_c^{(2)}(r'_1, r'_2 | r_1, r_2) \\ = R_c^{(2)}(r'_1, r'_2 | r_1, r_2) \\ + \frac{1}{2} \{ \Gamma^{(1)}(r'_1 | r_1) R_c^{(1)}(r'_2 | r_2) + \Gamma^{(1)}(r'_2 | r_2) R_c^{(1)}(r'_1 | r_1) \\ - \Gamma^{(1)}(r'_1 | r_2) R_c^{(1)}(r'_2 | r_1) - \Gamma^{(1)}(r'_2 | r_1) R_c^{(1)}(r'_1 | r_2) \}. \quad (4.9)$$

The calculation of  $n$ -EDM reduces to the calculation of connected  $k$ -EDMs with  $k \leq n$ . Equation (4.8) is also useful to approximate the higher-order EDMs in terms of the lower-order EDMs and RDMs. For example, by neglecting  $R_c^{(n)}$ , we can approximate  $R_c^{(n)}$  in terms of  $R_c^{(k)}$  and  $\Gamma^{(n-k)}$  with  $k < n$ .

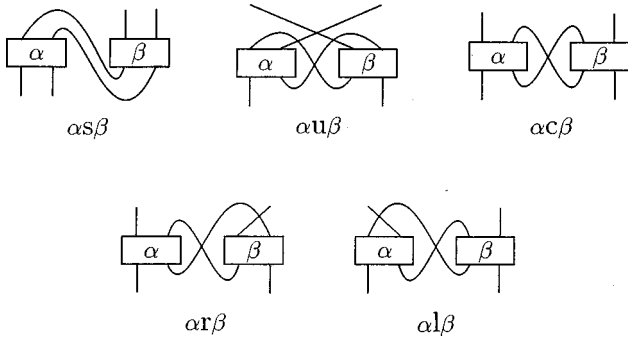


FIG. 2. Five connecting operations of  $s$ ,  $u$ ,  $c$ ,  $r$ , and  $l$  channels in Ref. [17].  $\alpha$  and  $\beta$  are the generic vertex diagrams. The operations of  $s_i$ ,  $u_i$ ,  $c_i$ ,  $r_i$ , and  $l_i$  with  $i=1,2$  are given by replacing one of the two internal  $G^{(1)}$  lines in the figures with the  $G_5^{(1)}$  line.

The connected 2-EDM can be calculated from the higher-order RDMs approximated with the method described in Sec. III. However, this method which constructs the 3- and 4-RDMs explicitly has two disadvantages. (i) Inclusion of the higher-order perturbation terms is difficult because the number of the distinct diagrams rapidly increases with the order of the perturbation as well as the order of the RDM increases. In particular, the systematic summation of physically important diagrams up to any orders is hopeless. (ii) It requires more computational time and resources than the direct calculation of EDM. In Sec. V, using the similarity of the diagrams between  $G_c^{(n)}$  and  $R_c^{(n)}$ , we construct a diagrammatic method to sum up the Parquet diagrams of the connected 1- and 2-EDMs.

## V. PARQUET EQUATION OF THE ENERGY DENSITY MATRIX

In the preceding section, we expressed EDM in terms of the connected EDMs and the RDMs, while the connected EDM is expressed with diagrams similar to the Feynman diagrams of the Green's function. The diagrammatic method in the GF theory enables us to sum up the selected, physically important diagrams [13]. Using the similarity of the diagrams between EDM and GF, we sum up the Parquet diagrams. The Parquet sum is one of the most powerful methods in GF theory and includes diagrams critical to any reasonable description of the many-body systems, for example, the particle-hole ring for Coulomb interaction in an extended system and the particle-particle ladder which tame hard-core interaction.

In the GF theory, the two-body Parquet sum constructs the two-body vertex  $V$ , which gives the connected piece of  $G^{(2)}$ , from the bare interaction and irreducible diagrams. An irreducible diagram is defined as the vertex diagram which cannot be separated into two disjointed vertex diagrams by breaking two internal lines. Any other diagrams can be constructed by joining the bare interaction and irreducible diagrams with five connecting operations,  $s$ ,  $u$ ,  $c$ ,  $r$ , and  $l$ . All the diagrams generated from the given irreducible diagrams constitute the Parquet sum. The Parquet equation in the GF theory was studied by Lande and Smith [17]. The five con-

TABLE II. Associativity relations of  $s$ ,  $u$ ,  $c$ ,  $r$ , and  $l$  operations given in Ref. [17]. These connecting operations are shown in Fig. 2.  $\alpha$ ,  $\beta$ , and  $\gamma$  are the generic vertex diagrams. The first row shows the relationship of  $\alpha s(\beta s \gamma) = (\alpha s \beta) s \gamma$ .

$X$	$\beta s \gamma$	$\beta u \gamma$	$\beta c \gamma$	$\beta r \gamma$	$\beta l \gamma$
$\alpha s X$	$(\alpha s \beta) s \gamma$				
$X s \alpha$	$\beta s(\gamma s \alpha)$				
$\alpha u X$		$(\alpha u \beta) u \gamma$			
$X u \alpha$		$\beta u(\gamma u \alpha)$			
$\alpha c X$			$(\alpha c \beta) c \gamma$	$(\alpha c \beta) r \gamma$	$(\alpha r \beta) c \gamma$
$X c \alpha$			$\beta c(\gamma c \alpha)$	$\beta c(\gamma l \alpha)$	$\beta l(\gamma c \alpha)$
$\alpha r X$		$(\alpha r \beta) r \gamma$			
$X r \alpha$			$\beta c(\gamma r \alpha)$	$\beta r(\gamma u \alpha)$	$\beta l(\gamma r \alpha)$
$\alpha l X$			$(\alpha l \beta) c \gamma$	$(\alpha l \beta) r \gamma$	$(\alpha u \beta) l \gamma$
$X l \alpha$		$\beta l(\gamma l \alpha)$			

necting operations are shown in Fig. 2, in which the incoming legs of the diagrams are bottoms and the arrows giving the direction of the propagator lines are suppressed. The exact  $G^{(1)}$  is used as a propagator, and the self-energy insertions are not included explicitly in the diagrams. The  $s$ ,  $u$ ,  $c$ ,  $r$ , and  $l$  connecting operations satisfy the associativity relationships in Table II. Using these relationships, Lande and Smith derived the integral equation for the two-body vertex of  $G^{(2)}$ . We use these relationships to derive the integral equations for the connected 2-EDM. We also use the approximation Eq. (3.6) to write the 2-EDM in terms of 2-RDM. The integral equations derived give the connected EDMs directly without explicitly constructing 3- and 4-RDMs.

We first consider the connected 2-EDM generated by  $W_{E5}$ . It is given by replacing an interaction line in the connected  $G^{(2)}$  with  $w(r, r') \delta(t) \delta(t')$  and then setting the time variables of the external lines to zero. We refer to the  $\Sigma_5$  as the self-energy  $\Sigma$  in which one interaction line is replaced with  $w(r, r') \delta(t) \delta(t')$ .  $G_5^{(1)}$  is similarly defined, which is also generated by  $W_{E5}$ . Using Dyson's equation,  $G_5^{(1)}$  is expressed as

$$G_5^{(1)}(x'_1 | x_1) = \int G^{(1)}(x'_1 | y_1) \Sigma_5(y_1 | y'_1) G^{(1)}(y'_1 | x_1) dy_1 dy'_1. \quad (5.1)$$

Each term in the connected 2-EDM under consideration is approximated by joining several two-body vertices  $V$  and the sum of the irreducible diagrams  $I$  with five operations. The lowest-order term of  $I$  is the two-body interaction  $w$  while the next order is the fourth-order of the electron correlations [13]. Since  $G^{(1)}$  contains interaction lines, the connected 2-EDM also contains the diagrams in which several vertices  $V$  are joined by several  $G^{(1)}$  lines and one  $G_5^{(1)}$  line. We calculate the direct diagram in which an internal chain of propagators connects the left incoming leg to the left outgoing leg. The third term of Eq. (3.3a) is an example of a direct diagram, while the fourth is an exchange diagram. The exchange diagram is constructed by crossing the outgoing legs.

We will pay attention to the diagrammatic structure of the equation and use the shorthand notation of  $s$ ,  $u$ ,  $c$ ,  $r$ , and  $l$  operations. The solution  $X$  of the integral equation

$$\begin{aligned}
S &= (X-S)sV + Vs(X-S) + Vs(X-S)sV + S_1, \\
U &= (X-U)uV + Vu(X-U) + Vu(X-U)uV + U_1, \\
T &= (X-T)cV + Vc(X-T) + Vc(X-T)cV + T_1 \\
&\quad + (X-T)rV + Vr(X-U) + Vc(X-T)rV \\
&\quad + (X-U)lV + Vl(X-T) + Vl(X-T)cV \\
&\quad + [Vl(X-T)]rV + [Vr(X-T)]cV + [Vr(X-T)]rV \\
&\quad + [Vu(X-T)]lV, \\
X &= I + S + U + T
\end{aligned} \tag{5.2}$$

gives the Parquet sum of the direct diagrams of the connected 2-EDM generated by  $W_{E5}$ , in terms of  $V, I, G^{(1)}$ , and  $G_5^{(1)}$ . The quantities  $S_1, U_1$ , and  $T_1$  are given by

$$\begin{aligned}
S_1 &= V(s_1 + s_2)V, \\
U_1 &= V(u_1 + u_2)V, \\
T_1 &= V(c_1 + c_2)V + V(r_1 + r_2)V + V(l_1 + l_2)V,
\end{aligned}$$

where  $s_1$  and  $s_2$  indicate two connecting methods of two vertices with  $G^{(1)}$  and  $G_5^{(1)}$  lines. The proof of Eq. (5.2) is given in Appendix B. The shorthand notation  $VsV$  represents the formula

$$\begin{aligned}
VsV &= \int V(x'_1, x'_2 | y_1, y_2) G^{(1)}(y_1 | y'_1) G^{(1)}(y_2 | y'_2) \\
&\quad \times V(y'_1, y'_2 | x_1, x_2) dy_1 \dots dy'_2
\end{aligned} \tag{5.3}$$

in which  $x$  and  $y$  denote the set of time, position, and spin coordinates. Note that the  $s, u, c, r,$  and  $l$  operations require the time integration.

We then rewrite Eq. (5.2) in terms of 1- and 2-RDMs. We first attach four external  $G^{(1)}$  legs to each term in  $X$  and set the time variables of the external legs to zero. Next, each  $G^{(1)}$  connecting two vertices is replaced with the rhs of Eq. (3.6), and the  $G_5^{(1)}$  is replaced with

$$\begin{aligned}
G_5^{(1)}(x'_1 | x_1) &\approx -i \int G^{(1)}(x'_1 | q) P(q | r') R_5^{(1)}(r' | r) \\
&\quad \times P(r | q') G^{(1)}(q' | x_1) dq \dots dr'.
\end{aligned} \tag{5.4}$$

$R_5^{(1)}(r' | r) = -iG_5^{(1)}(r' | r)$  is a 1-EDM generated by  $W_{E5}$ . The diagram of vertex  $V$  with four  $G^{(1)}$  legs is replaced with  $V_\Gamma$  of Eq. (3.8). Through this procedure,  $VsV$  becomes

$$\begin{aligned}
VsV &= \int V_\Gamma(r'_1, r'_2 | q_1, q_2) P(q_1 | q'_1) P(q_2 | q'_2) \\
&\quad \times V_\Gamma(q'_1, q'_2 | r_1, r_2) dq_1 \dots dq'_2
\end{aligned} \tag{5.3'}$$

which contains no time integration, in contrast to Eq. (5.3). In short, change  $V$  in Eq. (5.2) with  $V_\Gamma, G_5^{(1)}$  with  $PR_5^{(1)}P$ , and the definition of the five connecting operations from Eq. (5.3) to Eq. (5.3'). Solution  $X$  of Eq. (5.2) gives the Parquet sum of the direct diagrams of the 2-EDM generated by  $W_{E5}$ ,

in terms of 1- and 2-RDMs. This rewriting procedure is general and applicable to other EDM diagrams.

Connected 2-EDM generated by  $W_{E2}$  is given by replacing one perturbation potential  $\tilde{v}$  in the connected  $G^{(2)}$  with  $v(r, r')\delta(t)\delta(t')$ . We refer to  $G_2^{(1)}$  as  $G^{(1)}$  in which one perturbation potential  $\tilde{v}$  is replaced with  $v(r, r')\delta(t)\delta(t')$ . Each term in the direct diagrams of this connected 2-EDM is approximated by joining the several vertices with several  $G^{(1)}$  lines and one  $G_2^{(1)}$  line with  $s, u, c, r,$  and  $l$  operations. Addition of the  $R_2^{(1)} = -iG_2^{(1)}$  to the  $R_5^{(1)}$  yields this sum.

We then consider the 2-EDM generated by  $W_{E4}$ . Typical examples of the  $R_c^{(n)}$  diagrams generated by  $W_{E4}$  are shown in Figs. 1(d)–1(f). In Figs. 1(e) and 1(f), an incoming leg and an arbitrary internal position  $x'$  are connected with the line  $w(r, r')\delta(t')$ . Any  $R_c^{(2)}$  diagrams are classified into two kinds. Each diagram in the first kind is separated into the two diagrams containing  $w(r, r')\delta(t')$  and the vertex  $V$  by breaking one  $G^{(1)}$  line, such as Fig. 1(d) and some diagrams in Fig. 1(f). The sum of these direct diagrams is given as

$$\begin{aligned}
&\int G^{(1)}(r'_1 | x'_1) G^{(1)}(r'_2 | x'_2) V(x'_1, x'_2 | x_1, x_2) \\
&\quad \times G_4^{(1)}(x_1 | r_1) G^{(1)}(x_2 | r_2) dx_1 \dots dx'_2
\end{aligned} \tag{5.5}$$

and the corresponding term in which the left and right legs are changed.  $G_4^{(1)}$  denotes the 1-GF generated by  $W_{E4}$ ,

$$iG_4^{(1)}(x'_1 | x_1) = \lim_{J \rightarrow 0} \frac{\delta^2 W_{E4}}{\delta J^*(x'_1) \delta J(x_1)}. \tag{5.6}$$

Each diagram in the second kind cannot be separated into two diagrams with  $w(r, r')\delta(t')$  and without it by breaking one  $G^{(1)}$  line, such as Fig. 1(e) with  $k=1$  and the rest diagrams of Fig. 1(f). In these diagrams, an incoming leg and an internal position  $x'$  are connected with the interaction line  $w(r, r')\delta(t')$ . We approximated these diagrams by joining  $V$  and  $I$  with the  $s, u, c, r,$  and  $l$  operations. We consider the direct diagram whose left incoming leg  $r_1$  is connected to the internal line with  $w(r_1, r')\delta(t')$ . Other terms are obtained by changing the left and right legs and by crossing the outgoing legs.

Solution  $X$  of the equation

$$\begin{aligned}
S &= (X-S)sV, \\
U &= (X-U)uV, \\
T &= (X-T)cV + (X-T)rV + (X-U)lV, \\
X &= I + S + U + T,
\end{aligned} \tag{5.7}$$

gives the Parquet sum of these direct diagrams of the connected 2-EDM generated by  $W_{E4}$ , in terms of  $V, I,$  and  $G^{(1)}$ . The proof is given in Appendix C. We then rewrite Eqs. (5.5) and (5.7) in terms of 1- and 2-RDMs with almost the same procedure as in Eq. (5.2). We first attach three external  $G^{(1)}$  legs to each term in  $X$  and set the time variables of these external legs to zero. Each  $G^{(1)}$  connecting two vertices is then replaced with the rhs of Eq. (3.6), and the  $G_4^{(1)}$  is replaced with

$$G_4^{(1)}(x'_1|r_1) \approx \int G^{(1)}(x'_1|q_1)P(q_1|q'_1)R_4^{(1)}(q'_1|r_1)dq_1dq'_1. \quad (5.8)$$

$R_4^{(1)}$  denotes the 1-EDM generated by  $W_{E4}$ . The diagram of vertex  $V$  with four  $G^{(1)}$  legs is replaced with  $V_\Gamma$  of Eq. (3.8). In short, change  $V$  in Eq. (5.7) with  $V_\Gamma$ , and the definition of the five connecting operations from Eq. (5.3) to Eq. (5.3'), and solve Eq. (5.7). The sum of the solution  $X$  and the corresponding terms of changing the left and right legs, and crossing the outgoing legs, gives the Parquet sum of the 2-EDM generated by  $W_{E4}$ .

Finally, we consider the 1-EDM generated by  $W_{E5}$ , because other 1- and 2-EDMs are written with 1- and 2-RDMs. The 1-EDM

$$\begin{aligned} & 3 \int w(r_2, r_3) \Gamma^{(3)}(r'_1, r_2, r_3 | r_1, r_2, r_3) dr_2 dr_3 \\ &= - \lim_{J \rightarrow 0} \frac{\delta^2 W_{E5}}{\delta J^*(r'_1) \delta J(r_1)} + \Gamma^{(1)}(r'_1 | r_1) \text{Tr}\{w \Gamma^{(2)}\} \end{aligned}$$

can be calculated from the second term of the lhs of the equation,

$$\begin{aligned} & 3 \int \{w(r'_1, r_3) + w(r'_2, r_3)\} \Gamma^{(3)}(r'_1, r'_2, r_3 | r_1, r_2, r_3) dr_3 \\ &= \frac{1}{2} \lim_{J \rightarrow 0} \frac{\delta^4 (W_{E4} \exp W_G)}{\delta J^*(r'_1) \delta J^*(r'_2) \delta J(r_2) \delta J(r_1)}, \end{aligned}$$

by setting  $r'_2 = r_2$  and integrating this variable. By comparing these equations, we found the relationship

$$\begin{aligned} R_5^{(1)}(r'_1 | r_1) = & \int \left\{ R_{42}^{(2)}(r'_1, r_2 | r_1, r_2) \right. \\ & \left. - \frac{1}{2} R_4^{(1)}(r'_1 | r_2) \Gamma^{(1)}(r_2, r_1) \right\} dr_2, \quad (5.9) \end{aligned}$$

where  $R_4^{(1)}$  and  $R_5^{(1)}$  denote the 1-EDMs generated by  $W_{E4}$  and  $W_{E5}$ , respectively.  $R_{42}^{(2)}$  denotes the 2-EDM generated by  $W_{E4}$  and in which the right incoming leg  $r_2$  is connected to the internal line with  $w(r_2, r') \delta(t')$ . This term is already calculated with Eq. (5.7).

We summarize the calculation method of the Parquet sum of the 2-EDM in terms of the 1- and 2-RDMs. The 1-EDM generated by  $W_{E1} \dots W_{E4}$  and the connected 2-EDM generated by  $W_{E1}$  and  $W_{E3}$  are calculated from 1- and 2-RDMs directly. Direct diagrams of the connected 2-EDM generated by  $W_{E4}$  are given with the sum of Eq. (5.5) and the solution of Eq. (5.7). Other direct diagrams are obtained by changing the left and right legs. The 1-EDM  $R_5^{(1)}$  generated by  $W_{E5}$  is calculated with Eq. (5.9). The connected 2-EDM generated by  $W_{E5}$  is calculated with Eq. (5.2) from  $\Gamma^{(1)}$ ,  $V_\Gamma$ , and  $R_5^{(1)}$ . Finally 2-EDM is calculated from the 1-EDM, the connected 2-EDM, and the 1-RDM by Eq. (4.9).

In the present Parquet sum of 2-EDM, we introduced the approximation of Eq. (3.6). The lowest-order missing term due to this approximation is the second-order one, which represents the three-body cluster effect [4]. In the next sec-

tion, we approximate the irreducible diagram as  $w$  and omit the higher-order irreducible diagrams. Order analysis implies that the missing term due to Eq. (3.6) is more important than the higher-order irreducible diagrams. We can calculate the higher-order irreducible diagrams by the approximation of Eq. (3.6), and the missing term due to this approximation by the original GF method, as was discussed in Ref. [4].

## VI. DIRECT DETERMINATION OF THE DENSITY MATRIX

In Sec. V, we derived the integral equations for the Parquet sum of the 2-EDM. This infinite sum includes not only all the second-order perturbation terms of 3- and 4-RDMs already reported [4], but also many other higher-order terms such as the infinite sum of the ladder and bubble diagrams. In this section we examine the quality of the Parquet-sum method through the numerical calculations of atoms and molecules.

We first summarize our calculational method which is almost the same as the previous one [4], except that the 2-EDM is directly calculated without constructing the 3- and 4-RDMs explicitly. We solved the Hermite part of the second-order density equation [Eq. (1.1) with  $n=2$ ] in matrix form,

$$R_{j_1 j_2}^{i_1 i_2} + R_{i_1 i_2}^{j_1 j_2} = 0, \quad (6.1)$$

to calculate the spinless 2-RDM, imposing the normalization, Hermiticity, and the symmetry ( $D_{j_1 j_2}^{i_1 i_2} = D_{j_2 j_1}^{i_2 i_1}$ ) conditions on the 2-RDM. The subscript  $j_k$  and the superscript  $i_k$  are associated with the annihilation and creation operators, respectively. Because of the Hermiticity of the Hamiltonian, Eq. (6.1) is also equivalent to the Schrödinger equation, and we did not use the anti-Hermite part of the density equation. The spinless 2-RDM and the Hamiltonian were represented in matrices whose one-electron base are the HF orbitals. The generalized two-electron integrals were used for simplicity. We calculated the zeroth- and first-order terms of 2-EDM separately and summed the second- and higher-order terms with the integral equations of Eqs. (5.2) and (5.7), which were solved by the iterative method. We approximate the irreducible diagram as  $w$  and omit the higher-order irreducible diagrams. The multidimensional nonlinear equation (6.1) was solved by the same Newton's method as the previous one [4].

We applied the density-equation method to the following atom and molecules: Be,  $\text{NH}_3$ ,  $\text{CH}_4$ ,  $\text{N}_2$ , CO, and  $\text{C}_2\text{H}_2$  with the double- $\zeta$  basis [18] and  $\text{Li}_2$ ,  $\text{CH}_3\text{OH}$ ,  $\text{C}_2\text{H}_6$ ,  $\text{C}_3\text{H}_8$ , and  $\text{C}_4\text{H}_{10}$  with the minimal Slater-type orbital STO-6G basis [19]. We compared the accuracy of the present new approximation with the previous second-order one and the SDCI [20], full-CI [21] (in the case of relatively small basis sets), and the coupled-cluster single and double excitations with triple excitations included noniteratively [CCSD(T) for larger cases] [22]. Experimental molecular geometries [23] were used and some  $1s$  core orbitals of C and O were frozen.

Tables III and IV show the summary of the ground-state results. In Table III we compared the energies and the errors of the RDMs calculated by the Parquet-sum method with the second-order approximation, SDCI, and full-CI methods.

TABLE III. Energies and errors of the RDMs calculated by the density-equation methods and the wave-function methods. Parquet sum indicates the present new approximation, while some results of the second-order approximation are also presented in Ref. [4]. Errors of the RDMs are measured by the infinity norm. Numbers in square brackets indicate powers of 10.

Method	Density equation		Wave function	
	2nd order	Parquet sum	SDCI	Full-CI
Molecule	Energy (a.u.)			
Active	Correlation energy error (%)			
Electrons <sup>a</sup>	1-RDM error			
	2-RDM error			
NH <sub>3</sub>	-56.298 88	-56.303 14	-56.297 17	-56.304 33
4 × 10	4.24	0.92	5.58	0
8	4.72[-3]	4.67[-3]	9.86[-3]	0
	2.44[-2]	1.79[-2]	6.00[-2]	0
CH <sub>4</sub>	-40.295 82	-40.299 02	-40.294 05	-40.300 09
4 × 12	3.73	0.93	5.27	0
8	2.27[-3]	2.67[-3]	7.82[-3]	0
	1.79[-2]	1.24[-2]	4.78[-2]	0
CH <sub>3</sub> OH	-114.711 44	-114.715 84	-114.710 82	-114.718 16
7 × 5	5.24	1.81	5.72	0
14	5.12[-3]	4.03[-3]	1.42[-2]	0
	2.50[-2]	2.04[-2]	5.13[-2]	0
N <sub>2</sub>	-109.079 09	-109.096 36	-109.082 19	-109.106 05
5 × 11	11.84	4.26	10.48	0
10	9.85[-3]	2.87[-2]	2.79[-2]	0
	6.70[-2]	1.16[-1]	1.16[-1]	0
CO	-112.872 93	-112.885 25	-112.873 82	-112.895 09
5 × 11	10.55	4.68	10.13	0
10	1.87[-2]	1.47[-2]	4.14[-2]	0
	1.09[-1]	5.43[-2]	1.39[-1]	0

<sup>a</sup>The number of electrons in the active space.

The full-CI dimension of the CO molecule is about  $4.8 \times 10^6$ , which is the largest in Table III, while the number of the free parameters in the 2-RDM is about  $4.8 \times 10^3$ . In Table IV we compared the results with the CCSD(T) energies and CCD moments, because the full-CI calculations are currently difficult for these molecules.

As seen in these tables, the energies of the second-order approximation are comparable with the SDCI results, and those of the Parquet sum are comparable with the CCSD(T) or the exact results. The Parquet-sum method significantly improves the energies of all the molecules. Energy errors of the Parquet sum are about one-half to one-third of those of the second-order approximation for both singly bonded and triply bonded molecules. The correlation energy errors of the density-equation method are improved as the system becomes large, which is seen by comparing the results of the homologous series of alkanes, C<sub>2</sub>H<sub>6</sub>, C<sub>3</sub>H<sub>8</sub>, and C<sub>4</sub>H<sub>10</sub>. The fact that the energy errors from the full-CI or CCSD(T) energies are almost constant irrespective of the molecular size shows the size-consistent nature of the present density-equation method, because CCSD(T) is a good approximation of CCSDT, which is size-consistent.

In Table III we also compared the errors of the 1- and 2-RDMs measured by the infinity norm, which is the maximum row sum of the error matrix, while the row sum is calculated by adding the magnitudes of the elements in a

given row. The second-order approximation gives better RDMs than the SDCI method, while the Parquet sum gives the RDMs of accuracy similar to or better than the second-order approximation, except for the N<sub>2</sub> molecule. The Parquet sum may overcorrect the errors of the RDMs of the N<sub>2</sub> molecule, although it significantly reduces the energy error. The dipole moment of the CO molecule is a good test, because the Hartree-Fock method predicts the opposite direction [24]. The Parquet-sum method gives the dipole moment of 0.0691 a.u., which is slightly larger than the exact value of 0.0417 a.u. The second-order approximation and the SDCI give the dipole moments of 0.0344 and 0.0586 a.u., respectively. The Parquet-sum method yields a less accurate dipole moment than the second-order approximation, although it yields the 1-RDM of smaller error measured by the infinity norm.

In Table IV we compared the accuracy of the dipole or quadrupole moment. For the singly bonded molecules, the Parquet sum gives moments almost the same as, or slightly better than, those by the second-order method, and the results of both methods agree well with the exact one. For the C<sub>2</sub>H<sub>2</sub> molecule, the Parquet sum gives a slightly worse moment than the second-order method, although it significantly reduces the energy error.

We next applied the density-equation method to the excited states. Currently our program is applicable to the

TABLE IV. Energies and multiple moments calculated by the density-equation methods and the wave-function methods. Parquet sum indicates the present new approximation. Results are compared with CCSD(T) energies and CCD moments. Numbers in square brackets indicate powers of 10.

Method	Density equation		Wave function	
	2nd order	Parquet sum	SDCI	CCSD(T)
Molecule	Energy (a.u.)			
Active	Correlation energy error (%)			
Electrons <sup>a</sup>	Dipole or quadrupole moment (a.u.) <sup>b</sup>			
C <sub>2</sub> H <sub>6</sub>	-79.209 24	-79.213 18	-79.204 48	-79.214 49
7×7	3.45	0.858	6.58	0
14	0.4279	0.4290	0.4307	0.4298 <sup>c</sup>
C <sub>3</sub> H <sub>8</sub>	-118.228 68	-118.234 10	-118.215 59	-118.235 79
10×10	3.21	0.764	9.12	0
20	9.126[-3]	9.107[-3]	9.048[-3]	9.010[-3] <sup>c</sup>
C <sub>4</sub> H <sub>10</sub>	-157.249 73	-157.256 74	-157.224 69	-157.258 72
13×13	3.09	0.680	11.69	0
26	0.8021	0.8022	0.8130	0.8022 <sup>c</sup>
C <sub>2</sub> H <sub>2</sub>	-76.980 06	-76.987 08	-76.975 59	-76.994 97
5×15	7.61	4.03	9.89	0
10	4.642	4.486	4.817	4.628 <sup>c</sup>

<sup>a</sup>The number of electrons in the active space.

<sup>b</sup>Quadrupole moment is given in the case of the zero dipole moment.

<sup>c</sup>CCD moment.

closed-shell state, and we focused on the closed-shell, two-electron excited states of the Be atom and Li<sub>2</sub> molecule. The calculation method is the same as for the ground state. We used the double- $\zeta$  basis [25] for the Be atom and the minimal STO-6G basis [19] for the Li<sub>2</sub> molecule, and the experimental molecular geometry [23]. Table V shows the calculated results of two closed-shell excited states of the Be atom, and one closed-shell excited state of the Li<sub>2</sub> molecule. Because Be has four electrons, 4-RDM is essentially equivalent to the wave function, and the density-equation method is equivalent to the wave-function approach. On the other hand, the results of the six-electron system of the Li<sub>2</sub> molecule indicate the possibility of determining the excited-state 2-RDM by the functional approach.

As shown in Table V, the Parquet sum gives more accurate energies and 2-RDMs than the second-order method. Both methods give almost the same energies and density matrices as those of the SDCI method. Since the closed-shell two-electron excited state is often higher in energy than the open-shell one-electron excited state, the wave function cannot be approximated well with one Slater determinant, and the approximation of the RDMs is more difficult than the ground state. This explains why we could not calculate the RDMs of the excited states of other molecules. Li<sub>2</sub> with STO-6G basis is an exception: both the  $1^1\Sigma_g^+$  and  $8^1\Sigma_g^+$  states are well approximated with each Slater determinant, in which two valence electrons occupy  $\sigma(2s)$  bonding and  $\sigma^*(2p)$  antibonding orbitals, respectively. If we write the Hamiltonian as  $H=f+w_{\text{int}}$ , where  $f$  and  $w_{\text{int}}$  are the Fock operator and the correlation potential, and reduce the correlation potential to half,  $H=f+w_{\text{int}}/2$ , we can calculate the 2-RDMs of both the ground and excited states with the same symmetry by the density-equation method. This result suggests that the density-equation method can be applied to the

excited states if the proper functional for the excited state is used. In this approach, the orthogonalization condition of the wave functions is never explicitly imposed. These conditions will be satisfied automatically if we use the accurate functional, because our Hamiltonian is a Hermitian operator.

We examine some necessary conditions of the  $N$ -representability, the  $P$ ,  $Q$ , and  $G$  conditions [2], which are the non-negativities of the 2-RDM, 2-hole RDM, and the  $g$  matrix. Table VI shows the percentage of the sum of the negative eigenvalues of the  $P$ ,  $Q$ , and  $g$  matrices compared to the sums of their eigenvalues. This table shows that the calculated 2-RDMs contain nonrepresentable components, but the impurity fraction is small and around  $10^{-3}\%$  for both the ground and excited states. These fractions are almost constant or even become smaller as the molecule becomes large, which is seen by comparing the results of C<sub>2</sub>H<sub>6</sub>, C<sub>3</sub>H<sub>8</sub>, and C<sub>4</sub>H<sub>10</sub> molecules. The Parquet sum improves the  $N$ -representability of the 2-RDMs for singly bonded molecules, and their deviations are almost always smaller than the corresponding second-order results. For the triply bonded molecules, some are improved and others are not. A small deviation from the exact  $N$ -representability is due to an inaccuracy of the decoupling approximation of the RDMs. We also point out that all the 1-RDMs calculated by the density-equation method satisfied the ensemble representability condition: all the eigenvalues lie in the range of zero to two [2].

We then discuss various iterative methods used in the density-equation method. Since the ground-state 2-RDM is the zero-temperature limit of the finite-temperature 2-RDM, the limit  $\beta \rightarrow +\infty$  of the solution of the differential equation (2.2) gives the ground-state 2-RDM. Hence the discretization of the differential equation of Eq. (2.2),

$$\Gamma^{(2)}(\beta + \Delta\beta) \approx \Gamma^{(2)}(\beta) - \Delta\beta R^{(2)}(\beta), \quad (6.2)$$

TABLE V. Energies and errors of 2-RDMs of the ground and excited states calculated by the density-equation method. Parquet sum indicates the present new approximation.

Method	Density equation		Wave function	
	2nd order	Parquet sum	SDCI	Full-CI
State	Energy (a.u.)			
Main	Energy error (a.u.)			
config. <sup>a</sup>	2-RDM error (Euclidean norm)			
Be atom				
Ground	-14.582 70	-14.582 69	-14.582 69	-14.582 69
1.00(2200)	-1.54[-5]	2.53[-6]	4.06[-6]	0
	4.68[-5]	4.06[-5]	1.14[-4]	0
3 <sup>1</sup> S	-11.762 90	-11.762 86	-11.754 00	-11.762 86
1.00(2020)	-3.54[-5]	-1.92[-7]	8.86[-3]	0
	1.47[-4]	1.25[-4]	2.14[-2]	0
6 <sup>1</sup> S	-3.056 04	-3.056 04	-3.053 47	-3.056 01
0.99(0220)	-4.29[-5]	-2.81[-6]	2.54[-3]	0
	2.74[-4]	2.19[-4]	3.87[-2]	0
Li <sub>2</sub> molecule				
8 <sup>1</sup> Σ <sub>g</sub> <sup>+</sup>	-14.032 29	-14.033 48	-14.035 02	-14.036 25
1.00	3.97[-3]	2.78[-3]	1.23[-3]	0
(220...02)	7.77[-2]	2.95[-2]	7.15[-2]	0
Li <sub>2</sub> (1/2 correlation potential <sup>b</sup> )				
1 <sup>1</sup> Σ <sub>g</sub> <sup>+</sup>	-11.396 81	-11.399 18	-11.399 28	-11.399 28
1.00	2.47[-3]	1.08[-4]	3.58[-6]	0
(2220...0)	3.58[-2]	2.49[-3]	2.97[-4]	0
8 <sup>1</sup> Σ <sub>g</sub> <sup>+</sup>	-10.393 39	-10.393 66	-10.393 44	-10.393 70
1.00	3.03[-4]	3.79[-5]	2.58[-4]	0
(220...02)	2.16[-3]	2.97[-4]	3.12[-2]	0

<sup>a</sup>CI coefficient and electron occupations in the Hartree-Fock orbitals.

<sup>b</sup>Correlation potential of Li<sub>2</sub> molecule is reduced to half.

in which  $\Delta\beta$  is a small ‘‘time’’ step, yields the iterative method for the ground state. Valdemoro and co-workers and Mazziotti used similar methods [3,5], and Mazziotti analyzed the iterative method in connection with the power method. The structure of the statistical operator implies that the wavefunction component with energy  $E_i$  in 2-RDM grows at the rate of  $e^{-\Delta\beta(E_i-E_0)}$  by propagating a single time step  $\Delta\beta$ , where  $E_0$  is the ground-state energy of the fermion system. If the approximate functional does not yield the components with energies lower than  $E_0$  in the 3- and 4-RDMs, the iterative method of Eq. (6.2) converges. On the other hand, if the approximate functional yields the non- $N$ -representable components of lower energies, and does not decrease the fractions of the components at a rate less than  $e^{\Delta\beta(E_i-E_0)}$ , this iterative method diverges. According to our experience, the simple iterative method of Eq. (6.2) is unstable and difficult to converge, even for the small-enough  $\Delta\beta$ . Hence we used Newton’s method which is stable and behaves well, but requires more computational time. Since it may be an obstacle to apply the density-equation method to large systems, a more efficient iterative method must be devised.

Recently, Mazziotti applied the density-equation method to the quasispin model which is a nice benchmark for testing many-body theory, with as many as 40 particles by using his original approximation [5]. While the special symmetry of the model makes it possible to calculate the exact solution by diagonalizing the matrix of dimension  $(N+1)$ , the model

has a nontrivial solution and reproduces the difficulty of the correlation problem. Mazziotti contracted Valdemoro’s 4-RDM functional with our previous second-order correction for the 4-RDM [the fourth term of Eq. (3.3c)] to generate a system of equations for the 3-RDM. From a given 2-RDM, this system of equations yields the 3-RDM which is correct through second order. It significantly improves the accuracy of Valdemoro’s 3-RDM functional. In his scheme, the approximated 4-RDM automatically contracts to the 2-RDM from which it was made.

Mazziotti also proposed the ‘‘ensemble representability method’’ (ERM) to reconstruct the  $p$ -RDM from the 2-RDM without an explicit functional. The ERM requires that the  $p$ -RDM contracts to the 2-RDM, and also it satisfies the  $p$ -ensemble representability restriction that the  $p$ -RDM be Hermitian, antisymmetric, and positive semidefinite. Since these conditions are only necessary for  $N$ -representability when  $p$  is less than the number of the electrons, the solution is not unique and a family of solutions including the exact  $p$ -RDM results. He compared the accuracy of the 4-RDMs reconstructed by the ERM with his functional approach. The ERM is less accurate for the ground state than his reconstruction functional, but more accurate for the excited states.

These two reconstruction methods together with the second-order density equation were applied to the quasispin model [5]. These methods yield the ground-state energies and the 2-RDMs comparable to or better than those of SDCI.

TABLE VI. Percentage of the sums of the negative eigenvalues of the 2-RDM, 2-HRDM, and  $g$  matrix compared to the sums of their eigenvalues. Parquet sum indicates the present approximation. Numbers in square brackets indicate powers of 10.

Molecule Active <sup>a</sup>	Method	2-RDM	2-HRDM	$g$ matrix
Ground state				
CH <sub>4</sub>	2nd order	9.67[−3]	2.45[−4]	1.07[−3]
4×12	Parquet	1.66[−3]	0	9.52[−4]
C <sub>2</sub> H <sub>6</sub>	2nd order	3.52[−3]	2.34[−3]	1.46[−3]
7×7	Parquet	1.40[−5]	1.17[−2]	1.90[−4]
C <sub>3</sub> H <sub>8</sub>	2nd order	1.59[−3]	1.13[−3]	1.00[−3]
10×10	Parquet	2.60[−6]	3.67[−6]	1.40[−4]
C <sub>4</sub> H <sub>10</sub>	2nd order	1.16[−3]	8.70[−4]	1.05[−3]
13×13	Parquet	2.48[−7]	2.06[−6]	1.01[−4]
N <sub>2</sub>	2nd order	7.75[−3]	7.22[−4]	2.83[−3]
5×11	Parquet	4.05[−4]	1.24[−2]	3.61[−2]
CO	2nd order	5.85[−3]	5.28[−4]	7.21[−3]
5×11	Parquet	8.07[−5]	1.04[−3]	7.25[−3]
C <sub>2</sub> H <sub>2</sub>	2nd order	1.36[−2]	4.10[−4]	2.26[−3]
5×15	Parquet	4.65[−4]	1.45[−3]	1.04[−2]
Excited state				
Be (3 <sup>1</sup> S)	2nd order	6.39[−5]	9.70[−5]	1.89[−5]
2×2	Parquet	7.12[−5]	1.07[−4]	2.06[−5]
Li <sub>2</sub> (8 <sup>1</sup> Σ <sub>g</sub> <sup>+</sup> )	2nd order	1.69[−1]	3.97[−3]	1.93[−1]
3×7	Parquet	7.57[−2]	4.61[−4]	7.34[−2]

<sup>a</sup>Active space used in the calculation.

The ERM also yields the energy of the excited state with the same symmetry as the ground state. The energy was calculated somewhat lower than the exact energy. He also applied the third-order density equation with his functionals of the 4- and 5-RDMs to the quasispin model.

The ERM with the second-order density equation may be viewed as the density-equation method which uses the 4-RDM as a basic variable. Harriman suggested that such a method yields highly degenerated incorrect solutions at almost all the energies, unless enough  $N$ -representability restrictions are imposed [10] because of the indeterminacy of the equation. It is surprising that the ERM yields the energies and the 2-RDMs comparable to or better than SDCI by imposing very few conditions. There are some questions that must be clarified in the ERM, for example the dependence of the solution on the calculation algorithm, the extent of the nonuniqueness of the solution, and the applicability to other systems such as atoms and molecules. However, the ERM's possibility to yield the exact solution without any complicated functional is very attractive. Judging from the results of the quasispin model, we feel that his method seems to be very hopeful, and we anticipate the results of other systems, such as atoms and molecules.

## VII. CONCLUSIONS

In this paper we discussed methods to determine the second-order reduced density matrix (2-RDM) of the ground and excited states, finite-temperature systems, and large systems without using the wave function by solving the density

equation. We discussed the foundations to reconstruct the higher-order RDMs in terms of the lower-order ones. We presented a new equation for the direct determination of the RDMs of the finite-temperature canonical ensemble and showed that only the exact RDMs satisfy this equation. We reformulated our previous approximation method for 3- and 4-RDMs and examined the accuracy of the approximation for the excited states. The structure of the energy density matrix was analyzed by the generating-functional technique. Using the similarity of the diagrams between the Green's function and EDM, we derived the integral equations which sum up the Parquet diagram of the 2-EDM without explicitly constructing the 3- and 4-RDMs. This new approximation together with the second-order density equation was applied to the ground states of some molecules. The energy errors of the previous approximation were significantly reduced, giving almost the same energy as the exact or CCSD(T) one. We also calculated the closed-shell excited states of the Be atom and Li<sub>2</sub> molecule. The present density-equation method gave more accurate results than the SDCI method. We discussed the relationship between the iterative method and the finite-temperature density-equation method.

This paper reported the direct calculational method of the Parquet sum of 2-EDM, which is the first step in applying the density-equation method to large systems such as polymers and metals. The method based on the density matrix can be applied to large systems more easily than the wave function approach. In large systems the off-diagonal elements of 1-RDM and the vertex part of 2-RDM can be approximated as zero, if we use the localized one-electron basis. Hence we can calculate the 2-EDM with the computational time which scales linearly to the system size, by only skipping the calculation of the negligible off-diagonal elements. Although the calculational method of the 2-EDM with linear system-size scaling is trivial, a new stable iterative method whose computational time also scales linearly must be devised to apply the density-equation method to large systems. In this paper we also discussed methods to determine the RDMs of the excited states and the finite-temperature systems. To make these methods practicable, new approximate functionals for the 3- and 4-RDMs are necessary which are accurate enough for these systems.

## ACKNOWLEDGMENTS

The author acknowledges Professor H. Nakatsuji for his continuous encouragement and helpful comments. The English correction was made at the ITE technical English division. Some preliminary work in Tables I and V was carried out for the doctoral thesis at Kyoto University.

## APPENDIX A: DERIVATION OF THE FERMI DISTRIBUTION FUNCTION

We will show that Löwdin's formula for  $n$ -RDM [9],

$$\Gamma^{(n)} = \frac{1}{n!} \begin{vmatrix} \Gamma(r'_1|r_1) & \cdots & \Gamma(r'_1|r_n) \\ \vdots & & \vdots \\ \Gamma(r'_n|r_1) & \cdots & \Gamma(r'_n|r_n) \end{vmatrix}, \quad (\text{A1})$$

together with the first-order equation of Eq. (2.2) yields the Fermi distribution function for the noninteracting system.

We denote 1-RDM as  $\Gamma$  in this appendix. After a short calculation, we obtain the equation in matrix form,

$$-\partial_\beta \Gamma_j^i = v_j^k \Gamma_k^i - \Gamma_j^k v_k^l \Gamma_l^i. \quad (\text{A2})$$

Using the Hermiticity of  $\Gamma$  and  $v$ , we obtain the following equation:

$$v_j^k \Gamma_k^i - \Gamma_j^k v_k^i = [v, \Gamma]_j^i = 0 \quad (\text{A3})$$

which indicates  $v$  and  $\Gamma$  have coeigenfunctions for each  $\beta$ . We represent  $v$  and  $\Gamma$  as the diagonal matrices and their eigenvalues  $\epsilon_i$  and  $\gamma_i$ . Therefore

$$\gamma_i = (1 + e^{\beta \epsilon_i - c})^{-1}, \quad (\text{A4})$$

where  $c$  is a constant, satisfies Eq. (A2). If we write the constant  $c = \beta \mu$ , we get a Fermi distribution function. Although Löwdin's formula is valid only for the Slater determinant wave function, and the approximated RDMs do not give the original 1-RDM of finite temperature, we obtain the correct solution.

## APPENDIX B: PROOF OF EQ. (5.2)

We want to sum up two kinds of diagrams.

(1a) The diagrams in which several two-body vertices  $V$  and one irreducible diagram  $I$  are connected with  $s$ ,  $u$ ,  $c$ ,  $r$ , and  $l$  operations.

(1b) The diagrams in which several two-body vertices  $V$  are connected with  $s$ ,  $u$ ,  $c$ ,  $r$ , and  $l$  operations, and also in each diagram, one of the  $G^{(1)}$  lines linking two vertices is replaced with  $G_5^{(1)}$ .

Since  $V$  is the sum of all the direct vertex diagrams,  $V$  has any diagrams in  $VxV$  where  $x$  represents one of the five connecting operations. Hence any diagrams having a factor of  $VxV$  can be thrown away.

Consider the diagram in which an irreducible diagram and two or more vertices are connected with the five operations. Because this diagram is reducible, we can separate a vertex by breaking two  $G^{(1)}$  lines. However, we cannot separate the irreducible diagram, because if we could, the diagram in which the vertices are connected with five operations are left, and by assumption there are no such diagrams.

Next we consider the diagrams with three or more vertices in the set (1b). Because this diagram is reducible, we can separate a vertex by breaking two  $G^{(1)}$  lines, but we cannot separate a vertex by breaking the  $G^{(1)}$  and  $G_5^{(1)}$  lines for the same reason.

We then analyze the  $s$ -channel equation. Similar proof holds for the  $u$ -channel equation. The following two sets contain all the  $s$ -reducible diagrams we want to sum up more than once, together with the forbidden diagrams with a factor of  $VxV$ .

(2a) Diagrams of  $\alpha sV$  and  $Vs\alpha$  in which we can separate a vertex by breaking two  $G^{(1)}$  lines.  $\alpha$  is either the irreducible, or the reducible diagram in sets (1a) and (1b).

(2b) Diagrams of  $Vs_1V$  and  $Vs_2V$ , where  $s_1$  and  $s_2$  denote two connecting methods of two vertices by  $G^{(1)}$  and  $G_5^{(1)}$  lines.

Since the set (2b) is added to the equation explicitly, we will show that all the distinct diagrams we want to sum up in (2a) are contained in  $(X-S)sV$ ,  $Vs(X-S)$ , and  $Vs(X-S)sV$ .  $X$  denotes the Parquet sum which contains irreducible and reducible diagrams.  $S$  denotes the sum of the  $s$ -reducible diagrams in  $X$ . We first note that no diagram appears more than once in these three sets, because Table II shows that there is no way to rewrite them. These three sets contain any  $s$ -reducible diagrams of  $\alpha sV$  and  $Vs\alpha$ . Consider the diagram  $\alpha sV$ . If  $\alpha$  is irreducible, or reducible in one of the  $u$ ,  $c$ ,  $r$ , and  $l$  operations,  $\alpha sV$  is contained in  $(X-S)sV$ . If  $\alpha$  is  $s$ -reducible,  $\alpha = Vs\beta$  and  $\beta$  must not be  $s$ -reducible, because in other cases,  $\alpha sV$  has a factor of  $VxV$ . Hence  $\alpha sV$  is contained in  $Vs(X-S)sV$ . Diagram  $Vs\alpha$  is similarly treated. We demonstrated that the sum of  $(X-S)sV$ ,  $Vs(X-S)$ ,  $Vs(X-S)sV$ , and  $V(s_1+s_2)V$  gives all the  $s$ -reducible diagrams.

Next we analyze the  $t$ -channel equation. The following two sets contain all the  $c$ ,  $r$ , and  $l$ -reducible diagrams we have to sum up.

(3a) Diagrams of  $\alpha xV$  and  $Vx\alpha$  ( $x=c, r, l$ ) where  $\alpha$  is either the irreducible diagram, or the reducible diagrams in sets (1a) and (1b).

(3b) Diagrams of  $Vx_iV$ , where  $x_i = \{c_i, r_i, l_i; i=1,2\}$  connects two vertices by  $G^{(1)}$  and  $G_5^{(1)}$  lines.

Since the set (3b) is added to the equation explicitly, we will consider set (3a). Thirteen kinds of diagrams in Eq. (5.2),  $(X-T)cV, \dots, [Vu(X-U)]IV$ , are disjoint, since Table II shows that no diagrams can be transformed into each other. These thirteen kinds of diagrams contain any  $c$ -,  $r$ -, and  $l$ -reducible diagrams. Consider the diagram  $\alpha cV$ . If  $\alpha$  is irreducible, or reducible in  $s$ - or  $u$ -channel,  $\alpha cV$  is contained in  $(X-T)cV$ . If  $\alpha$  is  $r$ -reducible,  $\alpha = Vr\beta$  and  $\beta$  must not be  $u$ -reducible, and hence  $\alpha cV$  is contained in  $[Vr(X-U)]cV$ . If  $\alpha$  is  $l$ -reducible,  $\alpha = Vl\beta$  and  $\beta$  must not be reducible in the  $c$ ,  $r$ , and  $l$  channels; hence  $\alpha cV$  is contained in  $[Vl(X-T)]cV$ . Other diagrams of  $Vc\alpha$ ,  $\alpha rV$ ,  $Vr\alpha$ ,  $\alpha lV$ , and  $Vl\alpha$  are similarly treated. This completes the proof of Eq. (5.2).

## APPENDIX C: PROOF OF EQ. (5.7)

We want to sum up the distinct diagrams in which several vertices  $V$  and one irreducible diagram  $I$  are connected with  $s$ ,  $u$ ,  $c$ ,  $r$ , and  $l$  operations, and also the left incoming leg of the composite diagram is directly connected to the irreducible diagram. For the same reason as in Appendix B, we do not have to sum up any diagrams having a factor of  $VxV$ . Hence we can remove a vertex from the composite diagram by breaking two  $G^{(1)}$  lines, but we cannot remove the irreducible diagram. The diagram we want to sum has the form of  $\alpha xV$ , because in the diagram of  $Vx\alpha$ , the left incoming leg is not directly connected to the irreducible diagram. Consider the diagram  $(X-S)sV$ , where  $X$  denotes the sum of the Parquet diagrams and  $S$  denotes the sum of the  $s$ -reducible diagrams in  $X$ . No diagram appears more than once in this set, because Table II shows that there is no way to rewrite it. Hence we conclude that the sum of the  $s$ -reducible diagrams under consideration equals  $(X-S)sV$ . The same proof holds for  $u$ - and  $t$ -channel equations.

- [1] C. Garrod, M. V. Mihailovic, and M. Rosina, *J. Math. Phys.* **16**, 868 (1975); M. Rosina, B. Golli, and R. M. Erdahl, in *Density Matrices and Density Functionals*, edited by E. Erdahl and V. H. Smith, Jr. (Reidel, Dordrecht, 1987).
- [2] A. J. Coleman, *Rev. Mod. Phys.* **35**, 668 (1963); C. Garrod and J. Percus, *J. Math. Phys.* **5**, 1756 (1964); H. Kummer, *ibid.* **8**, 2063 (1967); R. McWeeny, *Rev. Mod. Phys.* **32**, 335 (1960); W. B. McRae and E. R. Davidson, *J. Math. Phys.* **13**, 1527 (1972); E. R. Davidson, *Chem. Phys. Lett.* **246**, 209 (1995); F. Sasaki, *Phys. Rev.* **138**, B1338 (1965); F. Weinhold and E. B. Wilson, *J. Chem. Phys.* **47**, 2298 (1967); T. L. Gilbert, *Phys. Rev. B* **12**, 2111 (1975).
- [3] F. Colmenero and C. Valdemoro, *Int. J. Quantum Chem.* **51**, 369 (1994); C. Valdemoro, L. M. Tel, and E. Pérez-Romero, *Adv. Quantum Chem.* **28**, 33 (1997).
- [4] H. Nakatsuji and K. Yasuda, *Phys. Rev. Lett.* **76**, 1039 (1996); K. Yasuda and H. Nakatsuji, *Phys. Rev. A* **56**, 2648 (1997).
- [5] D. A. Mazziotti, *Phys. Rev. A* **57**, 4219 (1998); *Chem. Phys. Lett.* **289**, 419 (1998); *Int. J. Quantum Chem.* **70**, 557 (1998).
- [6] S. Cho, *Ann. Rep. Gumma Univ.* **11**, 1 (1962); L. Cohen and C. Frishberg, *Phys. Rev. A* **13**, 927 (1976).
- [7] H. Nakatsuji, *Phys. Rev. A* **14**, 41 (1976).
- [8] P. Hohenberg and W. Kohn, *Phys. Rev.* **136**, B864 (1964); W. Kohn and L. J. Sham, *Phys. Rev.* **140**, A1133 (1965).
- [9] R. G. Parr and W. Yang, *Density-Functional Theory of Atoms and Molecules* (Oxford University Press, New York, 1989).
- [10] J. E. Harriman, *Phys. Rev. A* **19**, 1893 (1979). However, Mazziotti showed that such a method yields accurate result for the quasispin model. See Ref. [5].
- [11] C. Valdemoro, *Phys. Rev. A* **45**, 4462 (1992); F. Colmenero, C. Perez del Valle, and C. Valdemoro, *ibid.* **47**, 971 (1993); F. Colmenero and C. Valdemoro, *ibid.* **47**, 979 (1993).
- [12] M. Rosina, in *Reduced Density Operators with Application to Physical and Chemical Systems*, Queen's Papers in Pure and Applied Mathematics No. 11, edited by A. J. Coleman and R. M. Erdahl (Queen's University, Kingston, Ontario, 1968).
- [13] A. A. Abrikosov, L. P. Gor'kov, and E. Dzyaloshinskii, *Methods of Quantum Field Theory in Statistical Physics* (Prentice-Hall, Englewood Cliffs, NJ, 1963); J. W. Negele and H. Orland, *Quantum Many-Particle Systems* (Addison Wesley, New York, 1988).
- [14] V. A. Golovko, *Physica A* **230**, 658 (1996).
- [15] R. P. Feynman and A. R. Hibbs, *Quantum Mechanics and Path Integrals* (McGraw-Hill, New York, 1965).
- [16] J. Hubbard, *Proc. R. Soc. London, Ser. A* **240**, 539 (1957); C. Bloch, *Nucl. Phys.* **7**, 451 (1958); Y. S. Lee, S. A. Kucharski, and R. J. Bartlett, *J. Chem. Phys.* **81**, 5906 (1984); K. Raghavachari, *ibid.* **82**, 4607 (1985).
- [17] A. Lande and R. A. Smith, *Phys. Rev. A* **45**, 913 (1992).
- [18] T. H. Dunning, *J. Chem. Phys.* **53**, 2823 (1970).
- [19] W. J. Hehre, R. F. Stewart, and J. A. Pople, *J. Chem. Phys.* **51**, 2657 (1969).
- [20] M. Dupuis, A. Farazdel, S. P. Karna, and S. A. Maluendes, HONDO8.1, IBM Corporation.
- [21] P. J. Knowles and N. C. Handy, *Chem. Phys. Lett.* **111**, 315 (1984).
- [22] M. J. Frisch, G. W. Trucks, H. B. Schlegel, P. M. W. Gill, B. G. Johnson, M. A. Robb, J. R. Cheeseman, T. A. Keith, G. A. Petersson, J. A. Montgomery, K. Raghavachari, M. A. Al-Laham, V. G. Zakrzewski, J. V. Ortiz, J. B. Foresman, J. Cioslowski, B. B. Stefanov, A. Nanayakkara, M. Challacombe, C. Y. Peng, P. Y. Ayala, W. Chen, M. W. Wong, J. L. Andres, E. S. Replogle, R. Gomperts, R. L. Martin, D. J. Fox, J. S. Binkley, D. J. Defrees, J. Baker, J. P. Stewart, M. Head-Gordon, C. Gonzalez, and J. A. Pople, *Gaussian 94* (Gaussian Inc., Pittsburgh, PA, 1995).
- [23] L. E. Sutton, D. G. Jenkin, and A. D. Mitchell, *Tables of Interatomic Distances* (Chemical Society, London, 1958).
- [24] A. Szabo and N. S. Ostlund, *Modern Quantum Chemistry: Introduction to Advanced Electronic Structure Theory* (Macmillan, New York, 1982).
- [25] E. Clementi and C. Roetti, *At. Data Nucl. Data Tables* **14**, 428 (1974).